Nonlinear trans-resonant waves, vortices and patterns: From microresonators to the early Universe

Sh. U. Galiev[a)]
Department of Mechanical Engineering, The University of Auckland, Private Bag 92019, Auckland 1, New Zealand

T. Sh. Galiyev
New Zealand Funds Management Limited, 23-29 Albert Street, Private Bag 92163, Auckland, New Zealand

(Received 2 January 2001; accepted 7 June 2001; published 31 August 2001)

Perturbed wave equations are considered. Approximate general solutions of these equations are constructed, which describe wave phenomena in different physical and chemical systems. Analogies between surface waves, nonlinear and atom optics, field theories and acoustics of the early Universe can be seen in the similarities between the general solutions that govern each system. With the help of the general solutions and boundary conditions and/or resonant conditions we have derived the basic highly nonlinear ordinary differential equation or the basic algebraic equation for traveling waves. Then, approximate analytic resonant solutions are constructed, which describe the trans-resonant transformation of harmonic waves into traveling shock-, jet-, or mushroom-like waves. The mushroom-like waves can evolve into cloud-like and vortex-like structures. The motion and oscillations of these waves and structures can be very complex. Under parametric excitation these waves can vary their velocity, stop, and change the direction of their motion. Different dynamic patterns are yielded by these resonant traveling waves in the x–t and x–y planes. They simulate many patterns observed in liquid layers, optical systems, superconductors, Bose–Einstein condensates, micro- and electron resonators. The harmonic excitation may be compressed and transformed inside the resonant band into traveling or standing particle-like waves. The area of application of these solutions and results may possibly vary from the generation of nuclear particles, acoustical turbulence, and catastrophic seismic waves to the formation of galaxies and the Universe. In particular, the formation of galaxies and galaxy clusters may be connected with nonlinear and resonant phenomena in the early Universe.
[DOI: 10.1063/1.1394190]

Perhaps, Da Vinci first understood that surface water waves, sound and light waves are all propagated according to the same laws. This idea is valid both for linear and nonlinear waves. Brilliant investigations of nonlinear body and surface waves in different physical, chemical, and biological systems have been made during the last two centuries. In particular, anomalous parametric surface waves were observed in the last decade. We have found that similar waves may be in different physical, astrophysical, and chemical systems. The generation and the evolution, form, and amplitudes of these waves depend on the competition between nonlinear, dissipative, dispersive, and spatial effects inside trans-resonant bands. Due to this competition the waves in resonators may be compressed into chains of jets and spots, mushroom-like waves, vortices (Karman's "vortex street"), ellipsoidal-, and spiral-like structures. The velocity of the waves can depend on the parametric excitation. These effects are strictly localized in the resonant band and depend on the cavity detuning from resonance. They may be interesting for optoelectronics, quantum computing, telecommunication, etc. Further investigation of nonlinearities in the microresonators may open up new opportunities. In addition, highly nonlinear resonant effects can explain the amplification and the transformation of waves in large systems (e.g., earthquake-induced mountains, valleys, islands, etc.) and very large systems (e.g., the early Universe). Thus, the nonlinear, trans-resonant effects considered in this paper may be applied to different technologies and systems ranging from the atomic scale to the cosmos.

I. INTRODUCTION

The resonance is the classical problem with great practical impact in different natural, mechanical, physical, optical, electronic, and electrical systems. For simple mechanical systems, the resonant amplification and trans-resonant oscillations were considered beginning with Galileo Galilei. These phenomena were usually studied with the help of one degree of freedom or a few degrees of freedom models. According to the linear models the amplitude of the oscillations is infinite at the resonance. The amplitude is limited by nonlinear and/or dissipative effects. Sometimes, one degree of freedom or a few degrees of freedom models are too rough an approximation and wave properties must be taken into

a)Electronic mail: s.galiyev@auckland.ac.nz

account. The nonlinear resonant waves in infinite and finite mechanical systems have been studied for about 50 years.[1,2] The analogous resonant phenomena in optical and condensed matter systems are more recent developments, facilitated by advances in information technology and nanofabrication.[3–9]

The amplitude and the form of the resonant waves is defined by nonlinear, dispersive, dissipative, and spatial effects. In the trans-resonant frequency band a balance between these effects varies together with the frequency. Therefore inside the band unexpected phenomena can be generated. For example, the trans-resonant transformation of harmonic smooth waves into shock waves were observed in tubes.[2] In mechanical systems, only the first resonances can typically be observed, because of damping and the narrowing of the resonant band with increasing resonance number.[2] However, in electronic, optic, crystal, and quantum systems the damping may be very small and different resonances can occur. Electrons and atoms can form resonators. Interesting elliptic standing wave patterns were recently observed formed by a single atom and a two-dimensional free electron gas.[7,8] It was found[5] that the Bose–Einstein condensation can have unprecedentedly large nonlinearity. As a result, the resonantly tuned light pulses travel at a velocity of only 17 m/s and are strictly compressed in the condensation. This effect might explain various anomalous observations, in particular, in the cosmos. Indeed, the varying-speed-of-light theory of the cosmos was developed during recent years.[10] The acoustic resonant and nonlinear effects may be important for cosmology.[11–20] It has been discovered that the background radiation has large-size peaks (a fundamental mode) and smaller peaks (''overtones'').[20] The early Universe rang like a spherical resonator after the big bang. Thus, recent observations show that the acoustic model of the early Universe is correct. The rapid expansion of the Universe produced nonlinear pressure and density waves, since the matter of the early Universe was highly nonlinear and very dense.

One of the goals of this paper is to study highly nonlinear wave phenomena in various dissipative-dispersive resonant systems. These systems are surface layers, microresonators, the early Universe, etc. We develop the theory of trans-resonant wave phenomena in these systems. The perturbed wave equations are studied. It is known that physical processes of generation and transformation of waves can differ dramatically, nevertheless equations and analytical solutions describing these processes are often similar. For example, shock-, soliton- and cnoidal-like solutions are well known in nonlinear dynamics. In particular, it has been found recently that similar solutions describe waves in spherical resonators[23] and different anomalous wave phenomena, and wave patterns observed in water and granular layers.[21,22,24,25,27] It has been shown that the perturbed Maxwell wave equation and the perturbed Klein–Gordon field equation (ϕ^4 field) have similar solutions.[26] Here we develop the theory presented in Refs. 2 and 21–29.

The paper is organized as follows. In Sec. II the perturbed wave equations for different nonlinear systems are presented. It is shown in Sec. III that the same methods and assumptions enable us to obtain similar general approximate solutions of the perturbed wave equations [see, e.g., (25)]. Basic equations for the resonant waves are derived [see, e.g., (32)]. Trans-resonant effects, waves, and patterns are studied in Sec. IV. Analytical solutions are considered in Sec. IV A. They describe many wave phenomena and wave patterns, which have been observed recently in water and granular layers. In Sec. IV B the trans-resonant evolution of harmonic waves into particle- and cloud-like waves is studied with the help of the analytic solutions and numerical calculations. Effects of high nonlinearity and ''eddy'' viscosity are also treated. It was found that harmonic waves can amplify and evolve into mushroom-like waves and then into a cluster of vortices. This cluster is reminiscent of Karman's ''vortex street.'' On the other hand, we believe that the last process qualitatively simulates the nonlinear formation and growth of large-scale structures in the early Universe.[19] The particular solution $\mathrm{sech}^2(e \sin \zeta_-) \cos^2 \zeta_-$ [see (53) and (55)] is treated in Sec. IV C. It is known that this solution describes trans-resonant spherical waves[23] and some waves observed recently in surface layers.[21,22,24–28] We show that this solution describes the wave patterns observed recently in different microresonators, in Bose–Einstein condensations, and in electron structures. The summary and a brief discussion of the results may be found in Sec. V.

Thus, in this paper a wide spectrum of the resonant wave problems are treated. However, stochastic resonances[30] are not studied in this paper.

II. GOVERNING EQUATIONS

The equations under the consideration are presented in the following.

1D (one-dimensional) waves in strings, lattices and surface layers. The following equation may be valid for waves in one-dimensional objects:[24,27]

$$u_{tt} - a_0^2 u_{xx} = -gh_x + \beta u_x u_{xx} + \beta_1 u_x^2 u_{xx} + \beta_2 u_x^3 u_{xx} + \beta_3 u_x^4 u_{xx} + \mu u_{txx} + k u_{xxxx} + X + \beta_4 \tau_{31}, \tag{1}$$

where u is the longitudinal displacement, a_0 is the sound velocity, h is the thickness of objects, t and x are time and coordinate, respectively. Here and in the following letter subscripts denote differentiation with respect to the corresponding value. The first term on the right-hand side of (1) takes into account the variation of the thickness. Then there are quadratic, cubic, fourth- and fifth-order terms with regard to u. The dissipative (μu_{txx}) and dispersive ($k u_{xxxx}$) terms in (1) follow behind the nonlinear terms. X is a known function of the coordinate and the time, which defines the amplitude, and the motion of sources or initial ripples. The last term in (1) is defined by the surface friction. Coefficients in (1) can depend on t and x. This equation was derived for surface water, granular, and seismic waves.[24,27] In particular, some of Charles Darwin's seismic observations were simulated with the help of Eq. (1).[24,27] Versions of Eq. (1) can also describe nonlinear waves propagating in bubbly liquids, molecular and atomic lattices.[29,31] For further details the reader is referred to Refs. 22, 24–27, and 31.

The perturbed Maxwell wave equation. One-dimensional propagation of the electromagnetic waves E is described by[32]

$$E_{tt}-c_0^2E_{xx}=(a_1E+a_2E^2+a_3E^3+\mu E_t+kE_{xx})_{tt}+X+F, \tag{2}$$

where c_0 is the velocity of light, coefficients c_0, a_1, a_2, a_3 μ, and k may depend on t and x. Linear phenomenological dispersive $(\mu E_t)_{tt}$ and dissipative $(kE_{xx})_{tt}$ terms were added in (2). The dissipative phenomenological nonlinear third-order term F was also inserted in (4). This term will be defined in Sec. III B. Equation (2) gives opportunities to study the light propagation in spatially and temporally inhomogeneous media and microresonators. If c_0 is a function of t, then Eq. (2) describes parametric excited waves. Nonlinear Schrödinger-type equations follow from the perturbed Maxwell equation (2).[32]

Perturbed Klein–Gordon field equation. We shall consider the following form of this equation:

$$\phi_{tt}-c_0^2\nabla^2\phi=-c_0^2\beta_c^2\partial\Phi(\phi)/\partial\phi+\mu\nabla^2\phi_t+k\nabla^4\phi+X+F. \tag{3}$$

Here β_c is the Compton propagation constant. Different expressions for the function Φ can be found in Ref. 33. We assumed in (3) that $c_0=c_0(x,y,t)$, where x and y are rectangular coordinates. The phenomenological dispersive $(\mu\nabla^2\phi_t)$ and dissipative $(k\nabla^4\phi)$ terms were added in (3). In particle physics the Klein–Gordon equation represents the wave equation of a free relativistic particle. In this case we have $\beta_c=2\pi mc_0/h^*$, where m is the mass of the particle and h^* is Planck's constant. The Klein–Gordon equation also describes the motion of the field in very small structures and superconductors.[34–36] It is interesting that the Klein–Gordon equation may be reduced to the Schrödinger equation in the small-momentum limit.[36] On the other hand the Klein–Gordon equation can describe the waves in a crystal[31] (sine-Gordon equation) and it is also known in astrophysics.[37]

Cosmological perturbed wave equation. Some recent observations suggest that galaxies and galaxy clusters formed when the Universe was less than a billion years old.[17,18] Astronomers have trouble explaining how they formed so early on. It was assumed that the early Universe contained seeds of these structures.[18] In particular, the rapid expansion of the Universe immediately after the big bang should have produced waves traveling from pole to pole of the expanding spherical Universe. These waves now show up as ripples in the amount of background radiation.[19,20] Some astronomers[17–20] consider these waves as ''seeds,'' which later evolved into the large-scale structures of the cosmos. We need to study the evolution of these waves in order to understand the generation of galaxies, the formation of galaxy clusters, and the evolution of the Universe.

Cosmic structures have formed as a result of complex processes. During the last two decades, significant progress has been made in the numerical simulation of these processes. At the same time analytical models have been developed.[11–16] In this paper the nonlinear wave processes in the early Universe are studied with the help of analytical methods. In the early Universe the pressure p dominates over gravity. A convenient relativistic equation of state is $p=(\gamma_*-1)a_0^2\rho$, where $\gamma_*=\gamma_*(t)$ or a constant and ρ is density.[38] Usually, it was assumed that $\gamma_*>1$. At early times the speed of sound a_0 in the Universe was about the speed of light. In the considered case, the fluid equations in expanding coordinates are $\rho_t+3d^{-1}\ d_t\rho+d^{-1}\nabla(\rho\boldsymbol{\nu})=0$ and $\boldsymbol{\nu}_t+d^{-1}\boldsymbol{\nu}\nabla\boldsymbol{\nu}+d^{-1}d_t\boldsymbol{\nu}=d^{-1\rho-1}\nabla p$ [see Eqs. (9.15) and (9.17) from Ref. 14]. Here $d=d(t)$ is a scale factor describing the Hubble expansion of the Universe. We assume that d (t) is known. Then we introduce the velocity potential ψ: $\boldsymbol{\nu}=\nabla\psi$: As a result, after some algebra, the fluid equations are reduced to the following perturbed wave equation:

$$\begin{aligned}\psi_{tt}-c_*^2\nabla^2\psi=&-(1+d^{-1})\nabla\psi\nabla\psi_t-d^{-1}(\nabla\psi)^2\nabla^2\psi\\&+3c_*^2d_t+F+X-(d_td^{-1})_t\psi-d_td^{-1}\psi_t\\&-d_td^{-2}(\nabla\psi)^2-c_*^2d(c_*^{-2}d^{-1})_t\\&\times[\psi_t+0.5(\nabla\psi)^2+d_td^{-1}\psi].\end{aligned} \tag{4}$$

Here $c_*^2=(\gamma_*-1)a_0^2d^{-2}$. We inserted in (4) the functions X and F. Equation (4) is complex. Let us assume that d_t has the second order and $F=0$. In this case we have from (4) that

$$\psi_{tt}-c_*^2\nabla^2\psi=-(1+d^{-1})\nabla\psi\nabla\psi_t+3c_*^2d_t+X. \tag{5}$$

We eliminate the third-order terms in (5). Generally speaking, the equations of fluid dynamics can describe the evolution of acoustic waves in the Universe.[14] However, following Hu *et al.*[39] we believe that wave-type equations provide a more convenient way to study the nonlinear development of waves in the early Universe.

Spherical waves. The sphere is the simplest object where there is interaction of nonlinear and spatial effects. Here some equations for spherical radial waves are considered. First we write an equation of radial oscillations of gas spheres[23]

$$\psi_{tt}-a_0^2(\psi_{\xi\xi}+2\xi^{-1}\psi_\xi)=-(\gamma-1)a_0^{-2}\psi_t\psi_{tt}-2\psi_\xi\psi_{\xi t}+\mu a_0^{-2}\psi_{ttt}+X, \tag{6}$$

where ξ is the radial coordinate and γ is the adiabatic exponent. The equation for body waves propagating in a solid body is derived in Ref. 23,

$$\varphi_{tt}-a_0^2(\varphi_{\xi\xi}+2\xi^{-1}\varphi_\xi)=a_0^{-2}\varphi_t\varphi_{tt}-\varphi_\xi\varphi_{\xi t}+\mu a_0^{-2}\varphi_{ttt}+X, \tag{7}$$

where φ is the displacement potential. For the spherical waves the sine-Gordon equation yields

$$\phi_{\xi\xi}+2\xi^{-1}\phi_\xi-c_0^{-2}\phi_{tt}=\xi^{-2}\sin 2\phi+X. \tag{8}$$

Equation (8) describes some cosmological effects.[40] The early Universe was spherically symmetrical. Only after the breaking of the symmetry of the different cosmic structures, strings and sheets were formed.

Two-dimensional waves in sheets, lattices, and surface layers. The following 2D equation generalizes Eq. (1):

$$\varphi_{tt}-a_0^2\nabla^2\varphi=g(h_0-h)+\beta^*(\nabla^2\varphi)^2+\beta_1^*(\nabla^2\varphi)^3 + \mu\nabla^2\varphi_t+k\nabla^4\varphi+X+\beta_4^*\int \tau_{31}dx. \quad (9)$$

Here the integral takes into account a boundary friction of sheet surfaces. In particular, all Charles Darwin's seismic observations were simulated with the help of Eq. (9).[27] Details are given in Ref. 27.

Hyperbolic reaction-diffusion equation. This equation is written as[41]

$$n_{tt}-a_n^2n_{xx}=-\tau_*^{-1}n_t+\tau_*^{-1}F(n)+n_t\partial F(n)/\partial n, \quad (10)$$

where n is the density of particles, τ_*^{-1} is the mean collision time for chemical reactions, $a_n^2=\tau_*^{-1}D$ (D is the diffusion coefficient), and $F(n)$ is the source function corresponding to the reactive process.

Nonlinear Schrödinger equation. This equation may be derived from the nonlinear Maxwell wave equation, or the Klein–Gordon equation, or equations of gas dynamics.[42] Therefore all results, which will be presented in the following, are also valid for systems described by the Schrödinger equation.

We inserted in (2)–(7), (9) phenomenological terms. For simplicity we used the similar notations for these terms. However, in the different equations they can have different dimensions. Generally speaking, the above-mentioned model equations with variable coefficients can have quite different intrinsic characteristics, coefficients, and different solutions. However, it will be shown in the following that all of the above-mentioned equations also have a class of similar solutions, written with the help of two traveling waves. They are periodic and nonperiodic resonant wave solutions constructed without using the time–space separation method. The solutions describe forced, parametric-excited and free waves, and wave patterns, which have both classical and quantum-mechanical features.

III. GENERAL APPROXIMATE SOLUTIONS

A. Perturbation method and weakly nonlinear solutions

In this section it is shown that Eqs. (1)–(10) have similar approximate general solutions.

1D waves. First we briefly consider a method of solving applicable to all the above-mentioned equations. A solution of (1) will be obtained to demonstrate the method.

Equation (1) is rewritten, introducing the variables

$$r=a(t)-x, \quad s=a(t)+x, \quad (11)$$

where $a(t)\equiv a=a_0$. Then we assume that

$$u=u^{(1)}+u^{(2)}+u^{(3)}+u^{(4)}+u^{(5)}+\cdots, \quad (12)$$

where $u^{(1)}\gg u^{(2)}\gg u^{(3)}\gg u^{(4)}\gg u^{(5)}$. Following Refs. 24 and 27 and using (1) linear differential equations for $u^{(i)}$ ($i=1,2,...,5$) can be derived. For example, for $u^{(1)}$and $u^{(2)}$ we have that

$$4a_t^2u_{rs}^{(1)}+a_{tt}(u_r^{(1)}+u_s^{(1)})=0, \quad (13)$$

$$4a_t^2u_{rs}^{(2)}=\beta(u_s^{(1)}-u_r^{(1)})(u_{rr}^{(1)}-2u_{rs}^{(1)}+u_{ss}^{(1)}). \quad (14)$$

Let the approximate localized solution of Eq. (13) be

$$u^{(1)}=J(r)+j(s). \quad (15)$$

Solution (15) is valid only if $a_{tt}[J'(r)+j'(s)]\approx 0$, where the prime denotes the differentiation with respect to the appropriate variable r and s. Thus, we shall consider the case when $a_{tt}\approx 0$. For example, we can assume that $a_t=$ const or $a(t)$ is proportional to t^α, where $\alpha<2$ and $t\to\infty$. The other example is $a_t=\sin^n\omega t$, where $n\gg 1$. On the other hand, solution (15) may be valid for waves[24,25] oscillating inside of some regions x and t, where $J'(a-x)\approx -j'(a+x)$. Solution (15) is reminiscent of the d'Alembert-type solution, but here the velocity of waves $J(r)$ and $j(s)$ can be variable and depends on t.

Now substituting (15) into (14) and integrating, one can find that

$$u^{(2)}=J_2(r)+j_2(s)+\beta a_0^{-2}[r(j')^2-s(J')^2]/8+d_1, \quad (16)$$

where $J_2(r)$ and $j_2(s)$ are some arbitrary functions of integration, d_1 is a constant of integration, and $J=J(r)$ and $j=j(s)$. We assumed that $\beta a_0^{-2}=$const. Using (15) and (16) we can find $u^{(3)}$, and then $u^{(i)}$ ($i=4;5$). This process is described in Refs. 24 and 27, where surface waves were studied. The final expression of general approximate solution (12) is

$$\begin{aligned} u=&J+j+J_2(r)+j_2(s)+J_3(r)+j_3(s)+J_4(r)+j_4(s)\\ &+J_5(r)+j_5(s)-\frac{1}{4}\int\int a_0^{-2}[g(h_s-h_r)-\beta_4\tau_{31}-X]\\ &\times dr\,ds+d_1-\tfrac{1}{8}\beta a_0^{-2}[s(J')^2-r(j')^2]+\tfrac{1}{4}\mu a_0^{-1}\\ &\times(sJ''+rj'')+\tfrac{1}{4}ka_0^{-2}(sJ'''+rj''')+\tfrac{1}{32}\beta^2a_0^{-4}[s^2(J')^2J''\\ &+r^2(j')^2j'']+\tfrac{1}{12}(\beta_1a_0^{-2}-\tfrac{5}{8}\beta^2a_0^{-4})[r(J')^3+s(j')^3]\\ &+\tfrac{1}{16}\beta_2a_0^{-2}[r(j')^4-s(J')^4]+\tfrac{1}{20}\beta_3a_0^{-2}[r(j')^4+s(J')^4], \end{aligned} \quad (17)$$

where $J_i(r)$ and $j_i(s)$ are some arbitrary functions of integration ($i=3,4,5$). For simplicity, the interaction of opposite traveling waves was not taken into account in (16) and (17). This interaction was considered in Refs. 22, 24, 25, and 27.

The solution (17) contains the coefficients, which grow infinitely when $t\to\infty$. Following Refs. 23, 24, and 27 we can eliminate t from these coefficients using the arbitrary functions. For example, if we assume that $J_2(r)=\beta a_0^{-2}r(J')^2/8$, $j_2(s)=-\beta a_0^{-2}s(j')^2/8$ in (16), then the solution (16) yields

$$u^{(2)}=\beta a_0^{-2}(r-s)[(j')^2+(J')^2]/8+d_1. \quad (18)$$

After the elimination of t from the coefficients in (17) we have the following solution of (1):

$$u=J+j-\frac{1}{4}\int\int a_0^{-2}[g(h_s-h_r)-\beta_4\tau_{31}-X]dr\,ds+d_1$$
$$-\tfrac{1}{4}\beta a_0^{-2}x[(J')^2+(j')^2]-\tfrac{1}{2}\mu a_0^{-1}x(j''-J'')$$
$$-\tfrac{1}{2}ka_0^{-2}x(j'''-J''')+(\beta_1 a_0^{-2}/6-\beta^2 a_0^{-4}/16)x$$
$$\times[(J')^3-(j')^3]+\tfrac{1}{8}\beta^2 a_0^{-4}x^2[J''(J')^2+j''(j')^2]$$
$$-\tfrac{1}{8}\beta_2 a_0^{-2}x[(j')^4+(J')^4]$$
$$-0.1\beta_3 a_0^{-2}x[(j')^5+(J')^5]. \quad (19)$$

Solutions of Eqs. (2)–(10) were obtained with the help of the perturbation method. In the following some solutions are presented. One can see that these solutions resemble the solution (19). The expression for 1D weakly nonlinear electromagnetic fields in finite space is

$$E=J+j+d_1+0.5a_1x(1+0.25a_1)(j'-J')$$
$$-\tfrac{1}{2}\mu x(J''-j'')-\tfrac{1}{2}kx(J'''-j''')+\tfrac{1}{8}a_1^2x^2(J''+j'')$$
$$-\tfrac{1}{2}a_3x[(J^3)'-(j^3)']+0.25\int\int c_0^{-2}(X+F)dr\,ds. \quad (20)$$

For simplicity we put $a_2=0$ in (2). The general case of Eq. (2) was considered in Ref. 25.

3D and 2D waves. The perturbation method allows us to construct expressions for 3D and 2D wave fields. In particular, Eq. (6) yields[23]

$$\psi=\xi^{-1}(J+j)+d_1+0.5a_0^{-1}\xi^{-2}[(J+j)^2]'$$
$$-0.25(\gamma+1)a_0^{-1}\xi^{-1}\int\int\xi^{-1}(J'+j')$$
$$\times(J''+j'')dr\,ds+0.25\mu a_0^{-1}\xi^{-1}(sJ''+rj''), \quad (21)$$

where $J=J(a_0t-\xi)$ and $j=j(a_0t+\xi)$. A similar solution of Eq. (7) can be found in Ref. 23.

The approximate solution of the Klein–Gordon equation (3) was written for the ϕ^4 field ($\partial\Phi/\partial\phi=\phi-\phi^3$):[25]

$$\phi=J+j+d_1+0.5(k_1x+k_2y)\Big[k_{12}^{-2}\beta_c^2\Big(\int J\,dr-\int j\,ds$$
$$-\int J^3\,dr+\int j^3\,ds\Big)+\mu k_{12}c_0^{-1}(J''-j'')+kk_{12}^2c_0^{-2}(J'''$$
$$-j''')\Big]+0.25k_{12}^{-2}\int\int c_0^{-2}(X+F)dr\,ds. \quad (22)$$

The cosmological wave Eq. (4) yields the following approximate solution:

$$\psi=J+j+d_1-\tfrac{1}{2}(k_1x+k_2y)\{c_*^{-1}k_{12}[(J')^2-(j')^2]$$
$$-\tfrac{1}{3}c_*^{-2}k_{12}^2[(J')^3-(j')^3]\}+0.25k_{12}^{-2}\int\int c_*^{-2}$$
$$\times(X+F)dr\,ds. \quad (23)$$

For simplicity we have assumed that the right-hand side terms in (3 and (4) have the same order. It was assumed that $d=1$ in (4).

Some plane waves in sheets propagate according to the following solution[27] of Eq. (9):

$$\varphi=J+j+d_1+\tfrac{1}{6}(\beta^*)^2a_0^{-4}k_{12}^4(k_1x+k_2y)^2[(J'')^3+(j'')^3]$$
$$+0.5(k_1x+k_2y)\Big\{\beta^*a_0^{-2}k_{12}^2\Big[\int(J'')^2dr-\int(j'')^2ds\Big]$$
$$+\mu a_0^{-1}k_{12}(J''-j'')+ka_0^{-2}k_{12}^2(J'''-j''')$$
$$+k_{12}^4[\beta_1^*a_0^{-2}-\tfrac{2}{3}(\beta^*)^2a_0^{-4}]\Big[\int(J'')^3dr-\int(j'')^3ds\Big]\Big\}$$
$$+0.25k_{12}^{-2}\int\int a_0^{-2}\Big[X+\beta_4^*\Big(\int\tau_{31}dx\Big)\Big]dr\,ds. \quad (24)$$

In (22)–(24) we assumed that $J=J(r)=J[k_{12}a(t)-k_1x-k_2y]$, $j=j(s)=j[k_{12}a(t)+k_1x+k_2y]$, $k_{12}^2=k_1^2+k_2^2$, where k_1, k_2, and k_{12} are constants. We also assumed that $a_t^2\approx c_0^2$ in (22), $a_t^2\approx c_*^2$ in (23), and $a_t^2\approx a_0^2$ in (24). The interaction of waves $J(r)$ and $j(s)$ was not taken into account in (16)–(20) and (22)–(24). This interaction was considered in Refs. 22, 24, 25, and 27.

Remark. Thus, we have shown that the approximate weakly nonlinear solutions of Eqs. (1)–(10) may be written as

$$U=J+j+F^*(J,j), \quad (25)$$

where U corresponds to unknown functions of Eqs. (1)–(10) and F^* is a known nonlinear function of J and j. The last traveling wave functions are defined by boundary and initial conditions of a problem. In the following we consider wave problems for resonators.

B. Resonators and basic equation

Much research is devoted to nonlinear waves in resonators.[2,3] Quadratic and cubic nonlinear effects are treated. In particular, Chester[44] studied effects of the cubic nonlinearity and quadratic nonlinear dissipation (eddy formation) on the resonant oscillations of gas in an open-ended tube. Here we shall briefly discuss boundary problems for the spherical resonator[23,43] and elongate periodical systems.[3,21,24,26,27]

Spherical resonator. We will study waves excited by a simple-harmonic source of pressure, which has radius R_1 and is placed in a center of the sphere. It is assumed that a pressure source region is very small with respect to the excited wavelength. The other boundary ($\xi=R_2$) of the sphere is free. Therefore we have

$$P-P_0=-B\cos\omega t \quad (\xi=R_1); \quad P-P_0=0 \quad (\xi=R_2), \quad (26)$$

where $P-P_0=-\rho_0(\psi_t+0.5\psi_\xi^2-0.5a_0^{-2}\psi_t^2)+\mu\rho_0a_0^{-2}\psi_{tt}$ (see Ref. 23). Here ψ is defined by (21) and P_0, and ρ_0 are the undisturbed pressure and the density, respectively. Considering the linear problem we found the following resonant frequencies $\Omega_N=\pi Na_0(R_2-R_1)^{-1}$ ($N=1,2,3,...$). The linear solution is not valid inside of resonant bands, where $\omega=\Omega_N+b$. Here b is a trans-resonant parameter. Following Refs. 23 and 43 one can obtain the basic equation valid inside the resonant band:

$$a_0\omega^{-1}bf''-[a_0\omega^{-2}b^2(R_2-R_1)+\tfrac{1}{2}\mu]f'''+\tfrac{1}{2}(f')^2/R_1R_2$$
$$=\rho_0^{-1}BR_1(R_2-R_1)^{-1}\cos^2\tfrac{1}{2}\omega t, \quad (27)$$

where $f(a_0t-\xi+R_2)=J(a_0t-\xi)$. Equation (27) is the Burgers–Korteweg–de Vries type equation writing for the traveling wave. Different trans-resonant solutions of this equation are presented in Refs. 22–27. It can be seen that the equation describes the strong amplification of waves inside resonant band if two first terms in (27) are small enough. In particular, for the inviscid gas at the exact resonance we have the algebraic problem and $f'=\pm\sqrt{\rho_0^{-1}BR_2R_1^2(R_2-R_1)^{-1}}\cos\tfrac{1}{2}\omega a_0^{-1}(a_0t-\xi+R_2)$. According to this solution the spherical resonant periodical shock waves may be excited in inviscid gas.[2,23,43]

Thus, considering the spherical waves we have shown that the boundary resonant wave problem may be reduced to an ordinary differential equation or algebraic equation.

Elongate periodical systems. We shall consider waves having period $2L$ and boundaries where an unknown function (or the space derivative of this function) equals zero or varies according to a harmonic law. We assume that $j(r)=-J(r)$ in the solutions, if an unknown function equals zero at the first boundary. If the space derivative equals zero at this boundary, it is assumed that $j(r)=J(r)$. Thus, we have[21–27]

$$j(r)=J(r) \quad \text{or} \quad j(r)=-J(r). \quad (28)$$

The resonance occurs if the reverberating waves are in phase with each other. In this case, the function $J(s)$ may be expanded in Taylor's series at the second boundary:[2,21–27]

$$J(s)=J(r)+bJ'(r)+0.5b^2J''(r)+0.133b^3J'''(r)+\ldots. \quad (29)$$

For example, let the unknown function $U=0$ at boundaries. In this case using (25) and (28), (29) we may reduce the boundary problem to the following ordinary differential equation: $bJ'(r)+0.5b^2J''(r)+0.133b^3J'''(r)=F^*[J(r)]$. This equation is similar to (27). Thus, the general approximate solutions of Eqs. (1)–(10) allow us to reduce the boundary problems for trans-resonant processes to ordinary differential equations with respect to $J(r)$. These equations were written recently for waves in tubes,[21] surface waves,[22,24–27] spherical waves,[23,43] and electromagnetic and field waves.[26] Following Refs. 2, 21–27, 43, 44, and 46 we can write the general expression for these ordinary differential equations:

$$D_7J'''+D_2J'+D_4J''+D_1(J')^2+D_3(J')^3+D_5(J')^4$$
$$+D_6(J')^5+D_*J'J''+\int\int F\,dr\,ds=X^*+d_*, \quad (30)$$

where d_* is a constant. The coefficients D_i ($i=1,2,...,7$) and X^* can depend on the time, coordinates, and r. There is function F in (30). It is assumed that this function is defined by so-called "eddy" viscosity.[44–46] Let for the 1D surface waves (19) F be a nonlinear function of the velocity and the displacement. We assume that $\tau_{31}=(u|u|)_t$. As a result we have

$$\int\int F\,dr\,ds=\frac{1}{4}\beta_4\int\int a_0^{-2}\tau_{31}dr\,ds$$
$$=\frac{1}{4}\beta_4\int\int a_0^{-2}(u|u|)_t dr\,ds$$
$$=\frac{1}{4}\beta_4\int\int a_0^{-1}[(u|u|)_r+(u|u|)_s]dr\,ds$$
$$\approx-\frac{1}{4}\beta_4a_0^{-1}\left(\int bj'|bj'|ds+\int bJ'|bJ'|dr\right)$$
$$\approx-0.5\beta_4a_0^{-1}b|b|\int J'|J'|dr.$$

It is assumed that $a_0\approx$const. It is emphasized that (19) and (28), (29) were used here. Turbulence and the bottom friction are often described with the help of the "eddy" viscosity model.[45] Sometimes this nonlinear dissipative mechanism is strictly localized and may be introduced in boundary conditions. For example, with the help of this model, van Wijngaarden[46] and Chester[44] described the generation of eddies at the lip of the open end of the resonant tube. Perhaps, the "friction" of vacuum[47,48] and the generation of electromagnetic and optic eddy-like waves[18,35,49] may be simulated with the help of the above-mentioned strictly nonlinear friction law. We shall assume that the following expression is valid for all perturbed wave equations presented in Sec. II:

$$\int\int F dr\,ds=s_2\int J'|J'|dr. \quad (31)$$

In particular, for the 1D layer we have that $s_2=-0.5\beta_4a_0^{-1}b|b|$. As the result, (30) yields the following basic equation:

$$D_7J'''+D_4J''+D_2J'+D_1(J')^2+D_3(J')^3+D_5(J')^4$$
$$+D_6(J')^5+D_*J'J''+s_2\int J'|J'|dr=X^*+d_*. \quad (32)$$

One can see that the "eddy" viscosity effect depends on b. Thus, this effect varies in the trans-resonant band together with the frequency, and it can amplify for some value of b. The ordinary integral-differential equation (32) approximately simulates resonant properties of Eqs. (1)–(10) in the case of weakly nonlinear waves and (31). Different particular cases of Eq. (32) were considered in Refs 24, 25, and 44. In particular, Chester[44] wrote

$$-\cos(\omega r/a_0)=a_0\omega^{-1}d[(J')^3+3RJ'/2^{2/3}]/dr+s_2J'|J'|, \quad (33)$$

which follows from (32). Equation (32) is complex but simpler than Eqs. (1)–(10).

Coefficients in (32) are defined by a considered equation. One can find these coefficients using (19) or (20), or (21), or (22), or (23), or (24) and (28), (29). For example, for the gas sphere the coefficients D_i ($i=1,2,\ldots,7$), D_*, X^*, and d_* may be defined by a comparison of Eqs. (32) and (27), and we have $D_4=a_0\omega^{-1}b$, $D_7=-[a_0\omega^{-2}b^2(R_2-R_1)+\tfrac{1}{2}\mu]$, $D_1=R_1^{-1}R_2^{-1}$, $X^*=\rho_0^{-1}BR_1(R_2-R_1)^{-1}\cos^2\tfrac{1}{2}\times\omega a_0^{-1}r$, $D_2=D_3=D_5=s_2=d_*=0$ in (32).

Ordinary differential equation for the early Universe. Let us transform the 2D solution (23) into Eq. (32). We assume the following boundary conditions for the potential of velocity ψ: $\psi=0$ if $k_1x+k_2y=0$ or L. Solution (23) is inserted at the boundary conditions. Then, using (28), (29), and (31), one can obtain the following equation for some plane waves propagating in the early Universe:

$$bJ'+0.5b^2J''+0.133b^3J'''+\tfrac{1}{3}c_*^{-2}k_{12}^2L(J')^3+s_2\int J'|J'|dr = 0.25k_{12}^{-2}\int\int c_*^{-2}Xdr\,ds. \tag{34}$$

This equation is a particular case of Eq. (32).

Remark. We emphasize that inside the resonant band the coefficient D_2 (or b) is small or $D_2=0$ ($b=0$), which explains the amplification of the waves inside the resonant band. Thus, we found that the investigation of weakly nonlinear resonant waves described by (1)–(10) may be reduced to analysis of Eq. (32).

C. 2D resonant localized nonlinear waves

The perturbation method was based on the assumption that the nonlinear terms are smaller than the linear terms. This restriction is often not important if a considered equation is derived for weakly nonlinear waves. However, sometimes we must consider strongly nonlinear waves. Generally speaking, the velocity of these waves depends on the amplitude and the weak dispersion, and it may be different from the velocity of the linear waves. Let us consider these waves using the following variables:

$$\begin{aligned} r&=a(t)k_{12}-k_1(x)-k_2(y)-K_{12}(x,y),\\ s&=a(t)k_{12}+k_1(x)+k_2(y)+K_{12}(x,y). \end{aligned} \tag{35}$$

Here $k_1(x)$, $k_2(y)$, and $K_{12}(x,y)$ are unknown functions, which will be defined later [see (54) and (55)].

2D surface waves. As an example, Eq. (9) will be considered. Let us rewrite (9) using (35):

$$\begin{aligned} &k_{12}a_{tt}(\varphi_r+\varphi_s)+a_0^2(k_{1,xx}+K_{12,xx}+k_{2,yy}+K_{12,yy})\\ &\times(\varphi_r-\varphi_s)+\{k_{12}^2a_t^2-a_0^2[(k_{1,x}+K_{12,x})^2\\ &+(k_{2,y}+K_{12,y})^2]\}(\varphi_{rr}+\varphi_{ss})\\ &+2a_0^2[(k_{1,x}+K_{12,x})^2+(k_{2,y}+K_{12,y})^2]\varphi_{rs}\\ &=-g(h-h_0)+\beta^*(\nabla^2\varphi)^2+\beta_1^*(\nabla^2\varphi)^3\\ &\quad+\mu^*\nabla^2\varphi_t+k^*a_0^{-2}\nabla^2\varphi_{tt}+X+\beta_4^*\int\tau_{31}dx. \end{aligned} \tag{36}$$

We treat three cases of the resonant amplification of the waves.

(1) Let $\varphi_{rs}\approx 0$, $\varphi_r\approx\varphi_s\approx 0$, then we have resonance if

$$k_{12}^2a_t^2-a_0^2[(k_{1,x}+K_{12,x})^2+(k_{2,y}+K_{12,y})^2]=0. \tag{37}$$

(2) Let $\varphi_{rs}\approx 0$ and $a_{tt}\approx 0$, $k_{1,xx}\approx 0$, $k_{2,yy}\approx 0$, $K_{12,xx}\approx 0$, $K_{12,yy}\approx 0$, then we again have the resonant condition (37).

(3) In this case, we assume a set of the following resonant conditions:

$$\varphi_{sr}\approx\varphi_r\approx\varphi_s\approx 0,\quad a_t\approx k_{1,x}\approx k_{2,y}\approx K_{12,x}\approx K_{12,y}\approx 0. \tag{38}$$

If the above-mentioned resonant conditions occur, then Eq. (36) reduces to the following form:

$$\begin{aligned} g(h-h_0)&=\beta^*(\nabla^2\varphi)^2+\beta_1^*(\nabla^2\varphi)^3+\mu^*\nabla^2\varphi_t\\ &\quad+k^*a_0^{-2}\nabla^2\varphi_{tt}+X+\beta_4^*\int\tau_{31}dx. \end{aligned} \tag{39}$$

We note that the value $\nabla^2\varphi$ is proportional to the surface elevation.[27] Equation (39) is the ordinary differential *resonant* equation for $\nabla^2\varphi$. Thus, at the resonance, the problem again reduces to Eq. (32). If effects of the dissipation and the dispersion are very small, then we have the *resonant* algebraic equation for $\nabla^2\varphi$: $g(h-h_0)=\beta^*(\nabla^2\varphi)^2+\beta_1^*(\nabla^2\varphi)^3+X$.

The perturbed Klein–Gordon field equation. Let $\partial\Phi(\phi)/\partial\phi=\frac{3}{4}\phi^5-2\phi^3+\phi$ in (3).[33] As a result, in the above-mentioned case (1) or (2), or (3) Eq. (3) yields $c_0^2\beta_c^2(\frac{3}{4}\phi^5-2\phi^3+\phi)=\mu c_0^{-2}\phi_{ttt}+kc_0^{-4}\phi_{tttt}+X+F$, since $\phi_{tt}\approx c_0^2\nabla^2\phi$.

Cosmological perturbed wave equation (5). If one of the above-mentioned cases [(1), (2), or (3)] takes place we have from (5) that $(\nabla\psi)^2=\int(3c_*^2d_t+X)dt$. It was assumed that $d=1$ in (5).

Thus, it was shown in Secs. III B and III C that the central problem of this paper is reduced to studying Eq. (32). In the following we shall consider solutions, waves, vertices, and patterns yielded by (32).

We emphasize that coefficients in the above-mentioned ordinary differential and algebraic equations may be functions of r, s, x, y, or t.

IV. TRANS-RESONANT WAVES, VERTICES, AND PATTERNS

A. Analytic research of waves generated by Eq. (32)

Let us consider a case when D_5, D_6, s_2, X^* in (32) are zero and $D_7=1$. In this case we have the following cubic nonlinear equation:

$$J'''+D_2J'+D_4J''+D_1(J')^2+D_3(J')^3+D_*J'J''=d_*. \tag{40}$$

According to Refs. 24, 25, and 27 we shall seek the approximate solution of the last equation as a sum of traveling periodical waves

$$\begin{aligned} J'(r)&=B\tanh(e\sin\zeta_-)\cos^k\zeta_-\\ &\quad+A\,\mathrm{sech}^2(e\sin\zeta_-)\cos^K\zeta_-+C\cos^z\zeta_-, \end{aligned} \tag{41}$$

where $\zeta_-=\pi L^{-1}M^{-1}(r+c_-)$, A, B, C, e are unknown constants, k, K, and z are integers and c_- is an arbitrary constant. Expression (41) describes the interaction and the competition between the nonlinear, dissipative, and dispersive effects. In the limit cases, (41) simulates shock-, soliton-, cnoidal-, and harmonic-type waves. Thus, expression (41) describes all well-studied waves. Therefore, we shall consider (41) as *universal* wave functions. They define infinite spectra of waves because $M^{-1}=1,2,3\ldots$. In (41) r is defined by (35) [or (11)].

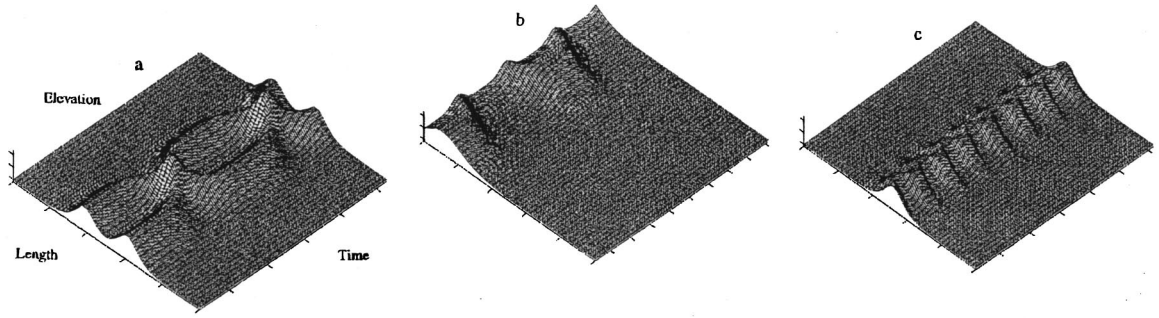

FIG. 1. Simulation of parametrically excited surface water waves (Ref. 50) with the help of solution (49): oscillations and the interaction of a pair of soliton-like waves ($c_{\pm}=L/2$, $k_{12}=2$, and $M=1$) (a); the interaction of a soliton and a boundary ($c_{\pm}=L/4$, $k_{12}=2$, and $M=2$) (b); the localization of the parametric harmonic excitation ($c_{\pm}=L/2$, $k_{12}=1/3$, and $M=1$) (c).

Therefore the wave functions (41) are not the d'Alembert-type wave functions, and for any cases the solution (41) describes a new kind of wave. It will be shown that (41) describes many interesting results of recent physical experiments.

Expression (41) is substituted into (40). Next, equating to zero nonlocalized terms, and terms containing $\mathrm{sech}^2(e\sin\zeta_-)$, or $\mathrm{sech}^4(e\sin\zeta_-)$ or $\tanh(e\sin\zeta_-)$ we obtain

$$C(D_2-z\pi^2L^{-2}M^{-2})\cos^z\zeta_- + D_1B^2\cos^{2k}\zeta_- + D_1C^2\cos^{2z}\zeta_- + 3D_3CB^2\cos^{2k+z}\zeta_- + D_3C^3\cos^{3z}\zeta_- = d_*, \tag{42}$$

$$A(D_2-K\pi^2L^{-2}M^{-2})\cos^K\zeta_- - 2Ae^2\pi^2L^{-2}M^{-2}\cos^{K+2}\zeta_- - D_1B^2\cos^{2k}\zeta_- + 2D_1AC\cos^{K+z}\zeta_- + D_4Be\pi L^{-1}M^{-1}\cos^{k+1}\zeta_- - 3D_3CB^2\cos^{2k+z}\zeta_- + 3D_3AC^2\cos^{K+2z}\zeta_- + D_*BCe\pi L^{-1}M^{-1}\cos^{z+k+1}\zeta_- = 0, \tag{43}$$

$$D_3A^3\cos^{3K}\zeta_- + 3D_3CA^2\cos^{2K+z}\zeta_- + D_1A^2\cos^{2K}\zeta_- + D_*ABe\pi L^{-1}M^{-1}\cos^{K+k+1}\zeta_- = 0, \tag{44}$$

$$B(D_2-k\pi^2L^{-2}M^{-2}+2D_1C\cos^z\zeta_-)\cos^k\zeta_- + D_3B^3\cos^{3k}\zeta_- + 3D_3BC^2\cos^{2z+k}\zeta_- = 0. \tag{45}$$

For fixed k, K, and z one can obtain algebraic equations for A, B, C, and e from (42) to (45). We emphasize again that the ordinary differential equation (40) and solution (41) define solutions for all equations (1)–(10). These solutions describe forced, parametric, and free waves. Here, as an example, parametric surface waves will be considered. The surface elevation η is defined by u_x (1D case) or $\nabla^2\varphi$ (2D case).

Following Ref. 25 we consider a few cases when coefficients in (41) may be easily found.

(I) Let $A=C=0$, $k=1$, and $d_*=D_1B^2/2$. In this case $B^2=4(\pi^2L^{-2}M^{-2}-D_2)/3D_3$ and $e=BMLD_1/\pi D_4$. Thus, quadratic nonlinear and viscous effects are taken into account. If $D_3=(\pi^2L^{-2}M^{-2}-D_2)/3$, then we have

$$\eta=2h[\tanh(e\sin\zeta_-)\cos\zeta_- + \tanh(e\sin\zeta_+)\cos\zeta_+]. \tag{46}$$

Here $\zeta_+=\pi L^{-1}M^{-1}(s+c_+)$ and c_+ is an arbitrary constant.

(II) Let $A=0$, $k=0$, $z=1$, and $D_1\approx D_*\approx 0$, $d_*=0$. In this case one can find that $B^2=(3\pi^2L^{-2}M^{-2}-2D_2)/8D_3$, $C^2=-(2D_2+\pi^2L^{-2}M^{-2})/4D_3$ and $e=3BCMLD_3/\pi D_4$. If $D_3=(3\pi^2L^{-2}M^{-2}-2D_2)/32$, then $B=\pm 2$ and we have the next expression for η:

$$\eta=h[2\tanh(e\sin\zeta_-)+C\cos\zeta_- + 2\tanh(e\sin\zeta_+) + C\cos\zeta_+]. \tag{47}$$

(III) Let $B=0$, $K=z=2$, and $d_*=0$. In this case one can find $A=-3C-6D_1/5D_3$ and $e^2=\pi^{-2}M^2L^2(2D_2/3-4\pi^2M^{-2}L^{-2}/3+D_1C+5D_3C^2/4)$, where $C=0$ or C is defined by the equation: $5D_3C^2+6D_1C+8D_2-16\pi^2M^{-2}L^{-2}=0$. Now we can write

$$\eta=h[A\,\mathrm{sech}^2(e\sin\zeta_-)+C]\cos^2\zeta_- + h[A\,\mathrm{sech}^2(e\sin\zeta_+)+C]\cos^2\zeta_+. \tag{48}$$

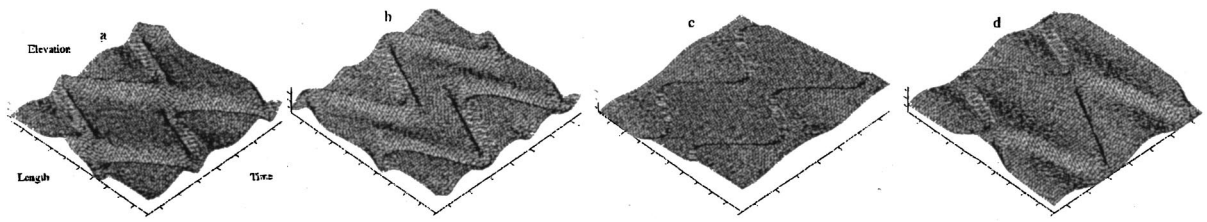

FIG. 2. Parametrically excited waves calculated according to solutions (46), (47) and (50) for $c_{\pm}=3L/4$, $k_1=2$, and $M=1$ [(a), (c), and (d)] and $c_-=3L/4$, $c_+=L/4$, $k_1=2$, and $M=1$ (b). Cases (a) and (b) describe oscillations and the interaction of surface water solitons observed in Ref. 51.

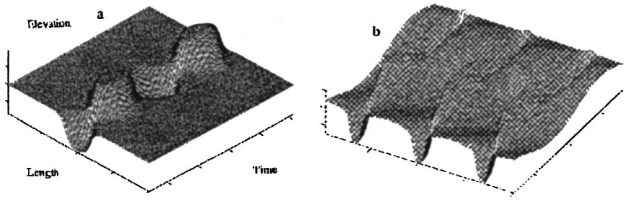

FIG. 3. Simulation of step-like standing surface oscillons excited in suspension (Ref. 53): single oscillon (a) and oscillon triad (b).

Let us consider a case when $C=0$ and $e\to\infty$. Then the wave transforms into a particle (jet) and we have approximately

$$\eta = hA[\operatorname{sech}^2(e\sin\zeta_-)\cos^2\zeta_- + \operatorname{sech}^2(e\sin\zeta_+)\cos^2\zeta_+]. \tag{49}$$

For liquid layers we have $A\approx 2$ in (49).

(IV) Let $D_1=0$, $B=0$, $K=z=1$, and $d_*=0$. In this case one can find $A=-3C$, $e^2=2-2\pi^{-2}M^2L^2D_2$, and $C^2=2(\pi^2M^{-2}L^{-2}-D_2)D_3^{-1}$. Now we can write

$$\eta = -hC[3\operatorname{sech}^2(e\sin\zeta_-)-1]\cos\zeta_- - hC[3\operatorname{sech}^2(e\sin\zeta_+)-1]\cos\zeta_+ . \tag{50}$$

For liquid layers we found[25] that $C=1.7(h/L)^{1/3}$ in (50).

Simulation of some experimental data by solutions (46), (47), (49) and (50). It was found[24,25] that solution (48) describes parametrically excited water and granular waves. Here we additionally consider some recently observed anomalous surface waves. Following Refs. 24 and 25 we calculated these waves using in (46), (47), (49), and (50) the expressions (41) and (11).

Some results of calculations according to solution (49) are presented in Figs. 1(a)–1(c). It was assumed that $a(t)=B_*k_{12}[\sin(\omega t/k_{12})-0.333\sin^3(\omega t/k_{12})]$. Here B_* is constant corresponding to experimental parameters. It can be seen that (49) describes all solitons observed in Ref. 50.

Figures 2 and 3 were calculated for $a(t)=a_0\omega^{-1}k_{12}\sin(\omega t/2)$. Pairs of positive and negative vibrating solitons observed in Ref. 51 on the water surface are simulated by solution (50) [Figs. 2(a) and 2(b)]. Figures 2(c) and 2(d) were calculated according to solutions (47) and (46), correspondingly. It is interesting that Fig. 2(d) resembles some results obtained recently for radiation-damped spin systems.[52]

We simulated experimental data[51] with the help of the perturbed wave equation (see also Refs. 24 and 25). It is important for our theory that these data are described also by the nonlinear Schrödinger equation.[51]

Let us consider experimental data[53] for parametric excited suspension layers. We assumed in (41) that $r=a_0\omega^{-1}\sin(\omega t/2)-k_1x$, $M=1$, and $c_-=L/2$, $c_+=-L/2$. Solution (47) ($C=0$ and $k_1=1$) and Fig. 3(a) describe the single oscillon presented in Figs. 1(a) and 1(b) from Ref. 53. The oscillon triad observed in Ref. 53 is simulated in Fig. 3(b). We used solution (46), where $k_1=3$. The reader can find further comparisons of observed anomalous liquid and granular waves and the solutions in Refs. 22 and 24–27.

Figures 1–3 were calculated using the experimental data. The opposite traveling waves form Figs. 1–3 [see (46), (47), (49), and (50)]. These waves form waves oscillating (Figs. 1 and 2) or fixed (Fig. 3) with respect to space points.

Thus, the parametric excitation allows us to keep the wave (in other words the information) inside the resonators. In particular, the harmonic excitation may be compressed into the particle-like waves. These waves can oscillate (Figs. 1 and 2) or stand (Fig. 3) inside of the resonator.

Radial symmetrical waves. At the resonance, 1D localized excitations may be excited in the systems according to Figs. 1–3. Let us consider the 3D (spherical) resonant waves. We used the following expression for the pressure:

$$P-P_0\approx-\rho_0\psi_t\approx-\rho_0a_0\xi^{-1}[J'(r)-J'(s)].$$

Here r and s are defined by (11) and (41). We considered the exact resonance and assumed $a(t)=a_0t$, $B=0$, $A=-3$, $C=1$, $K=z=2$, and $c_\pm=0$ in (11) and (41). Strictly localized waves may be excited in spherical resonators according to the calculations (see Fig. 4). These waves are defined by both number of the resonance (N) and number of the subharmonic mode (M). There is a strong amplification of the waves near $r=R_1$. One can see that the long harmonic wave radiated by the source [see (26)] strictly compresses and amplifies at the resonance.

B. Effects of high nonlinearity and "eddy" viscosity

We shall consider the following particular case of Eq. (32):

$$A_2(J')^5+A_1(J')^4+(J')^3+(3R/2^{2/3})J'+s_2\int J'|J'|dr + \cos\omega a_t^{-1}r=0, \tag{51}$$

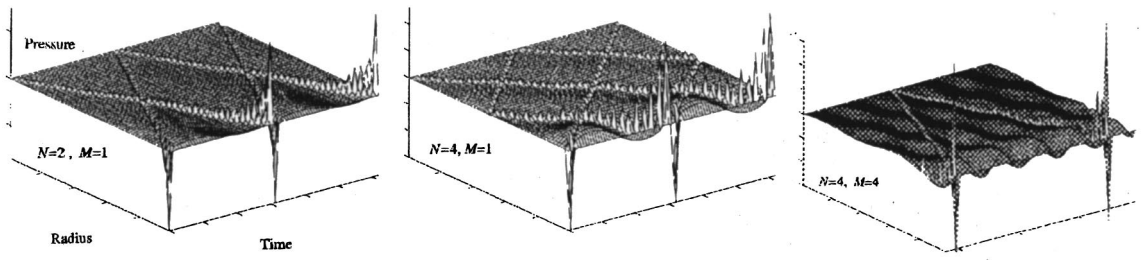

FIG. 4. Diverging and converging localized resonant pressure waves excited by a simple-harmonic source in the sphere. These waves are defined by both number of the resonance (N) and number of the subharmonic mode (M).

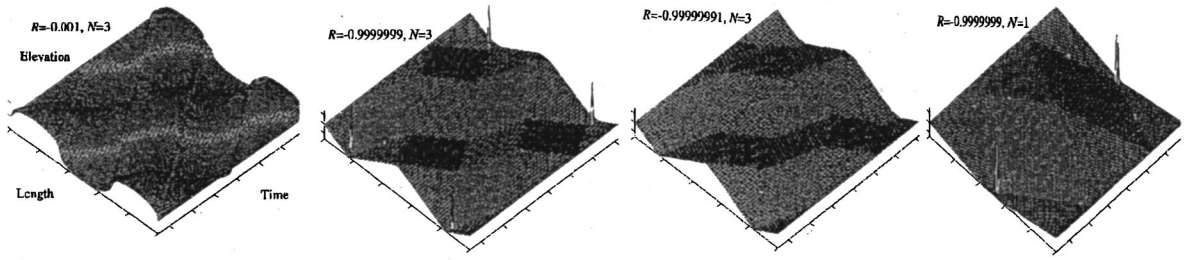

FIG. 5. The trans-resonant transformation of the shock-like waves into jet- and pyramid-like waves (R is trans-resonant parameter, N is number of the resonance) and the simulation of experimental data (Refs. 53 and 54).

where R is a trans-resonant parameter.[21–27] We have at the exact resonance that $R=0$. This equation generalizes the Chester equation (33). Equation (51) has one solution or three analytical solutions, if $A_1=A_2=s_2=0$. Using the three analytical solutions we can construct discontinuous and multivalued solutions. These solutions were used in Refs. 24 and 27 for studying the trans-resonant earthquake-induced oscillations of surface topographies. Here we shall use both analytical and numerical methods for studying waves and patterns generated by (51). Solutions of the Chester equation (33), and solutions of Eq. (51) rewritten for the inviscid medium ($s_2=0$) are compared. It will be shown that high nonlinearity can qualitatively describe the generation of vortices.

Waves and wave patterns described by analytical solutions. The trans-resonant transformation of the shock-like waves into pyramid-like waves is shown in Fig. 5. We use both the single-valued and multivalued analytical solutions, when R was near -1 or 0. Between these critical values of R there is only the multivalued solution of (51). Curves of Figs. 6, 7, 8(b) and 8(c) demonstrate the evolution of the analytical solutions and the waves at the section $x=L$. It is possible to give different interpretations of the curves. In particular, we shall treat the closed loops in the curves as vortex formations. In this case, Fig. 6 displays the generation ($R=-0.4$) and the trans-resonant evolution of a mushroom-like wave. It bifurcates into three surfaces when $R\approx-1$. Let us focus our attention on the last case. In Fig. 7 we qualitatively show that one structure of Fig. 6 ($R=-0.999\,99$) can bifurcate into loop- and vortex-like structures [Figs. 7(a) and 7(b)] or stable break-like waves [Fig. 7(c)], or pyramid- and jet-like waves.

One can see that Figs. 5–7 describe experimental data. The vertically excited pyramid- and jet-like waves [see Figs. 5 and 7(d)] on liquid and granular surfaces have been observed.[54–58] The shock- and/or step-like surface waves (Fig. 5) were excited in Ref. 53. The strip-like waves,[58] plumes, and mushroom-like waves with large heads were also studied.[59–61] Sometimes alternate-signed vertices were generated in the heads.[62] The jets [Fig. 7(d)] and the drops can form as the result of the interaction of these vortices [see Fig. 6 ($R=-0.999\,99$) and Refs. 61 and 62]. It was shown experimentally[56] and theoretically[25] that water mushroom-like waves, and jets (drops) can be generated due to vertical harmonic excitation. Indeed, according to Figs. 5–7 the harmonic excitation can generate surprising, very compressed, particle-like waves if $R\approx-1$. Apparently, these waves are Longuet-Higgins[54] excited with the help of vertical harmonic vibrations of a water layer.

Thus, in the trans-resonant regime the harmonic waves may be compressed into particle-like standing oscillating structures. The amount of these structures depends on the number of resonance (see Fig. 5).

Cubic nonlinearity, "eddy" viscosity, and generation of vortices. Following Ref. 44 we numerically solved Eq. (51) ($A_1=A_2=0$) for different s_2. For small s_2 the numerical solution was similar to the analytical solution inside the range $1>R>0$. However, the numerical solution was different from the analytical solutions inside the range $-1<R<0$ if s_2 was large enough. Figure 8, where the multivalued analytical and numerical solutions are compared, demonstrates this effect. On the other hand, Fig. 8 shows the correspondence of the close loops in Fig. 7 to the vortices. If s_2 is slightly larger than some critical value, which depends on R, then the mushroom-like waves having the vortex (spiral) pair appear in the trans-resonant band [see Fig. 8(a), cases $R=-0.5$, $s_2=0.26$, and $R=-0.9$, $s_2=-0.031$]. If s_2 increases further the spirals become tighter until they form nodal singularities [see Fig. 8(a) (cases $R=-0.5$, $s_2=0.5$ and $R=-0.9$, $s_2=-0.1$) and Ref. 44]. The singularities disappear and the numerical solution is continuous when s_2 is

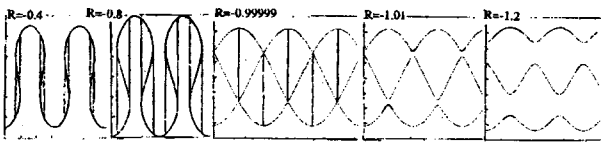

FIG. 6. Curves calculated acording to the analytical solution of equation $(J')^3+(3R/2^{2/3})J'+\cos\omega a_t^{-1}r=0$ demonstrating the generation ($R=-0.4$), the trans-resonant evolution ($R=-0.8$; $-0.999\,99$), and bifurcation ($R=-1.01$) of ripples. The cnoidal-type and saw-type (pyramid-type) waves may be generated as a result of the bifurcation. Three types of the harmonic waves may be generated in the system according to the analytical solutions outside of the resonant band ($R=-1.2$).

FIG. 7. A variety of wave structures which may be generated in the system: vortex-like waves (a), (b), breaking-like waves (c), and saw- and jet-like waves (d). They may be generated according to the analytic solution of equation $(J')^3+(3R/2^{2/3})J'+\cos\omega a_t^{-1}r=0$ if $R\approx-0.999\,99$.

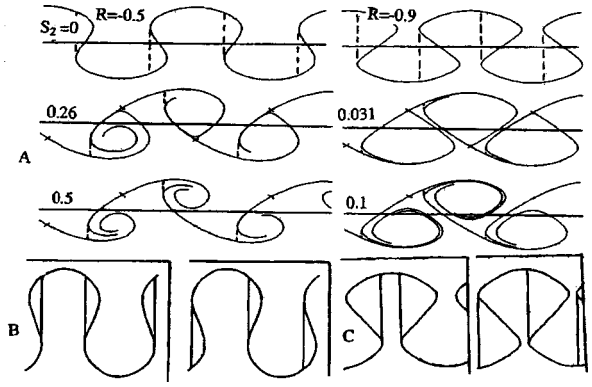

FIG. 8. Waves generated by equation $(J')^3+(3R/2^{2/3})J'+s_2\int J'|J'|dr+\cos\omega a_t^{-1}r=0$. Resonant and "eddy" viscosity effects on the trans-resonant evolutin of mushroom-like waves: numerical calculations (a) and analytical simulations (b), (c). Here R is the trans-resonant parameter and s_2 is the "eddy" viscous parameter. If in the resonant band s_2 is slightly larger than some critical value then the mushroom-like waves transform into the vortex pair.

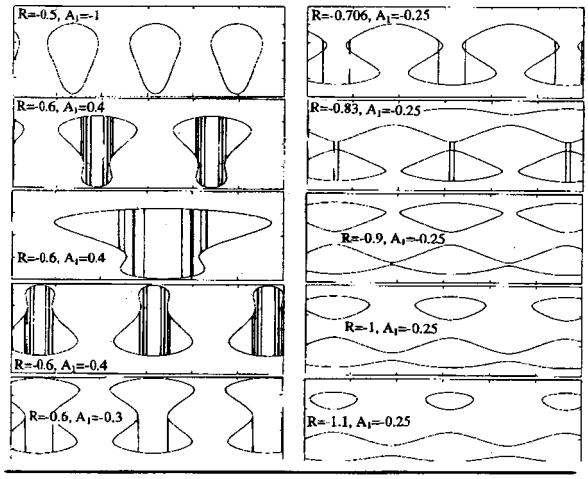

FIG. 10. Mushroom-like waves ($R=-0.708$ and $A_1=-0.25$) and the cloud-like structures are yielded by the fourth-order algebraic equation $A_1(J')^4+(J')^3+(3R/2^{2/3})J'+\cos\omega a_t^{-1}r=0$ inside and near the resonant band.

large enough. Let us consider the results of analytical solutions [Figs. 6, 7, 8(b) and 8(c)]. The solutions qualitatively describe the data of the numerical investigations, since we assumed that the loop pair corresponds to the vortex (spiral) pair.

Effects of high nonlinearity. In Figs. 9–13 we present results of a numerical soliton of (51). Let us consider cases when $A_1=A_2=s_2=0$ [Fig. 9(a)] and $A_1=s_2=0$, $A_2=-0.11$ [Figs. 9(b) and 9(c)] in Eq. (51). We assume that $R=0.03\omega r/a_0$, where $\omega r/a_0$ varies from -2 to -45 [Figs. 9(a) and 9(b)], or $R=-0.8+0.2\cos(\omega r/4a_0)$ [Fig. 9(c)]. One can see that the effect of high nonlinearity may be very important. The cubic nonlinearity generates loop-like structures which bifurcate into three harmonic curves when $R\approx-1$ [see Fig. 9(a) and Fig. 6]. These harmonic curves are tied by vertical lines. The fifth-order nonlinearity defines the more interesting picture [Fig. 9(b)]. The mushroom-like formations generate the ellipsoid-like clouds when $R\approx-1$. The fifth-order nonlinearity periodically generates these clouds [see Fig. 9(c)], if R oscillates near $R\approx-1$. More detailed results of the numerical calculations can be seen in Figs. 10–13. We assumed that $A_2=s_2=0$ (Fig. 10) and $A_1=s_2=0$ (Fig. 11) in (51). Figure 10 demonstrates a variety of cloud-like structures. Some of them simulate the shape of liquid drops bouncing on a solid surface.[63,64] There are different cloud-like structures in Fig. 11. One structure ($R=-0.81$, $A_2=-0.1095$) resembles the structure of Fig. 6 ($R=-0.8$). One can see the transformation of the complex structure ($R=-0.81$, $A_2=-0.1095$) into the Karman vortex street ($R=-0.81$, $A_2=-0.15$) (see also Fig. 7.10 in Ref. 61).

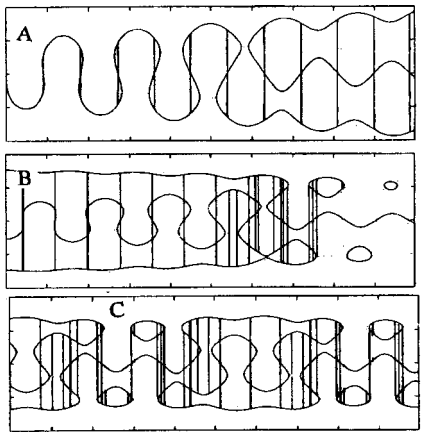

FIG. 9. The transition of ripples into mushroom-like waves and cloud-like structures calculated according to cubic equation $(J')^3+(3R/2^{2/3})J'+\cos\omega a_t^{-1}r=0$ (a) or fifth order equation $-0.11(J')^5+(J')^3+(3R/2^{2/3})J'+\cos\omega a_t^{-1}r=0$ [(b), (c)].

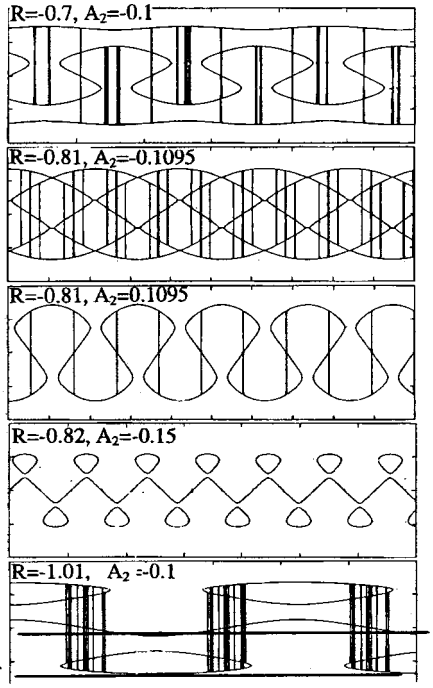

FIG. 11. Effect of the fifth-order nonlinearity on mushroom- and cloud-like structures calculated according to equation $A_2(J')^5+(J')^3+(3R/2^{2/3})J'+\cos\omega a_t^{-1}r=0$. The trans-resonant transformation of the mushroom-like waves ($R=-0.7$ and $A_2=-0.1$) into Karman's "vortex street" ($R=-0.82$ and $A_2=-0.15$; $R=-1.01$, and $A_2=-0.1$).

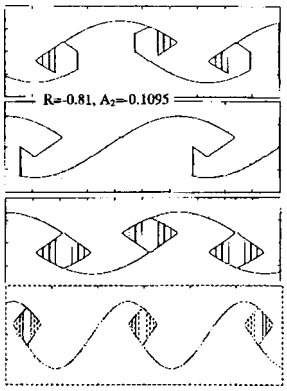

FIG. 12. Resonant mushroom- and breaking-like waves, and spiral-like structures generated by the fifth-order nonlinearity if $R \approx -1$.

Then in Fig. 12 we show that the complex structure from Fig. 11 ($R=-0.81$, $A_2=-0.1095$) contains mushroom- and break-like waves, and spiral structures.

Thus, under the simple harmonic excitation the systems can manifest very complex behavior. Changing the exciting term in (52) one can study an infinite variety[25] of wave phenomena in different systems.

We have considered the simple cases, when Eq. (32) is simplified to (51). In particular, Figs. 5–7 and 9–12 were calculated according to the algebraic equation. This equation does not take into account the influence of the dissipation and the dispersion. However, these figures qualitatively describe the observed evolution of ripples in the mushroom-like waves, vortices, and clouds.[65,66] Thus, it follows from the calculations that the influence of dissipation and dispersion on this evolution may be very small. It was also shown that in highly nonlinear media the ripples can be smoothly transformed and amplified into mushroom-like waves, spiral-, and ellipsoidal-like structures.

Turbulence may be generated by mushroom-like waves.[65,66] Therefore, turbulence can be generated even if the viscous effects are very small. We emphasize that the highly nonlinear spiral-like vortices in Fig. 12 are reminiscent of the vortices calculated for cubic nonlinear and the ''eddy'' friction [Fig. 8(a)]. Thus, the high nonlinearity can qualitatively simulate ''eddy'' viscosity and, perhaps, describe a generation of the wave turbulence. According to the theory this turbulence can weakly depend on the viscosity.

It is known that the front of turbulence can propagate like traveling waves.[67] This front may be formed by the traveling mushroom-like waves. These waves can generate the vortices when $R \approx -1$. Indeed, if $s_2=0$, Eq. (51) transforms into the algebraic equation. One has many (up to 5) real roots (see Figs. 9–11) if $R \approx -1$. These roots are located very close to each other. Therefore any noise can provoke the chaotic jumps and oscillations in the system if $R \approx -1$.[68,69]As the result, the wave turbulence may be generated.

Let us consider the transformation of harmonic ripples into the cluster of clouds (vortices). We assume in (51) that $A_1=s_2=0$, $A_2=-0.11$, and $R=0.0025\omega r/a_0 + \tanh(0.025\omega r/a_0)$, where $\omega r/a_0$ varies from 20 to -980. Results of calculations are presented in Fig. 13. One can see that ellipsoid-like clouds (vortices) are formed when

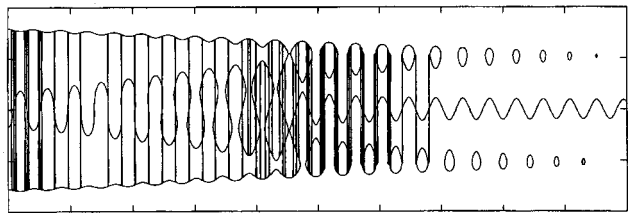

FIG. 13. Growth of ripples and the generation of mushroom-like waves, and a cluster of the clouds (vortices) are described by fifth-order algebraic equation $-0.11(J')^5+(J')^3+(3R/2^{2/3})J'+\cos \omega a_t^{-1} r=0$. Here parameter $R+R(t)$ varies from 0.4 to -1.25. The harmonic wave grows and transforms into shock-like and the mushroom-like wave, when $R(r)$ reduces from 0.4. The solutions bifurcate when $R(r) \approx -1$. As a result two rows of clouds (vortices) and the saw-like curve are generated. The vortices reduce and disappear when $R \approx -1.2$. Moreover, the saw-like curve transforms into the harmonic curve. This evolution is valid for all Eqs. (1)–(10). Perhaps, this figure qualitatively describes the evolution of ripples, the generation of galaxies and galaxy clusters in the early Universe.

$R \leqslant -1$. The clouds reduce together with R. They disappear when $R \approx -1.25$. As a result, we have the finite cluster of clouds (vortices).

It is possible to give a different interpretation of Figs. 9–13. For example, we can assume that Figs. 9(b), 9(c), and 13 simulate the generation of the Karman vortex street[61] (a sequence of alternate-signed traveling vortices arranged in two rows). On the other hand, one can treat Figs. 9(b), 9(c), and 13 as a sketch of the evolution of ripples of the density to vortex-like structures, which transit into ellipsoid galaxies.

Nonlinear and "eddy" effects in the early Universe. The last results are applicable to problems of the formation of galaxies and clusters of galaxies. Let us consider the ordinary differential equation (34) for the early Universe. Inside the resonant band b^2 and b^3 in (34) are very small. It has been found for (33) and (51) (see Figs. 6–13) that the mushroom-like waves and trans-resonant vortices can appear from ripples in nonlinear and dense enough media, if the critical condition $R \approx -1$ holds. The early Universe was very dense and highly nonlinear. Therefore, the mushroom-like waves and trans-resonant vortices could form there. On the other hand, in natural systems the condition $R \approx -1$ can occur during finite time and inside finite space. Therefore, the natural cluster of vortices forming in the trans-resonant regime cannot contain too many vortices. Indeed, the clusters of the Universe usually have hundreds of galaxies.[17] Thus, galaxies formed together with the cluster during short enough time and inside a rather small space. According to our theory the formation of a single galaxy is practically impossible.

C. Wave patterns governed by analytic solution (41)

Solutions (46)–(50) describe an infinite variety of waves and wave patterns which may be generated in nonlinear, dispersive–dissipative spatiotemporally inhomogeneous systems. Of course, it is impossible to study all of them. Some 1D and 2D systems were considered in Refs. 24, 25, and 27. Here we continue the consideration of 2D patterns.

We shall consider the patterns generated by expressions $J'(r)+J'(s)$, where according to (49)

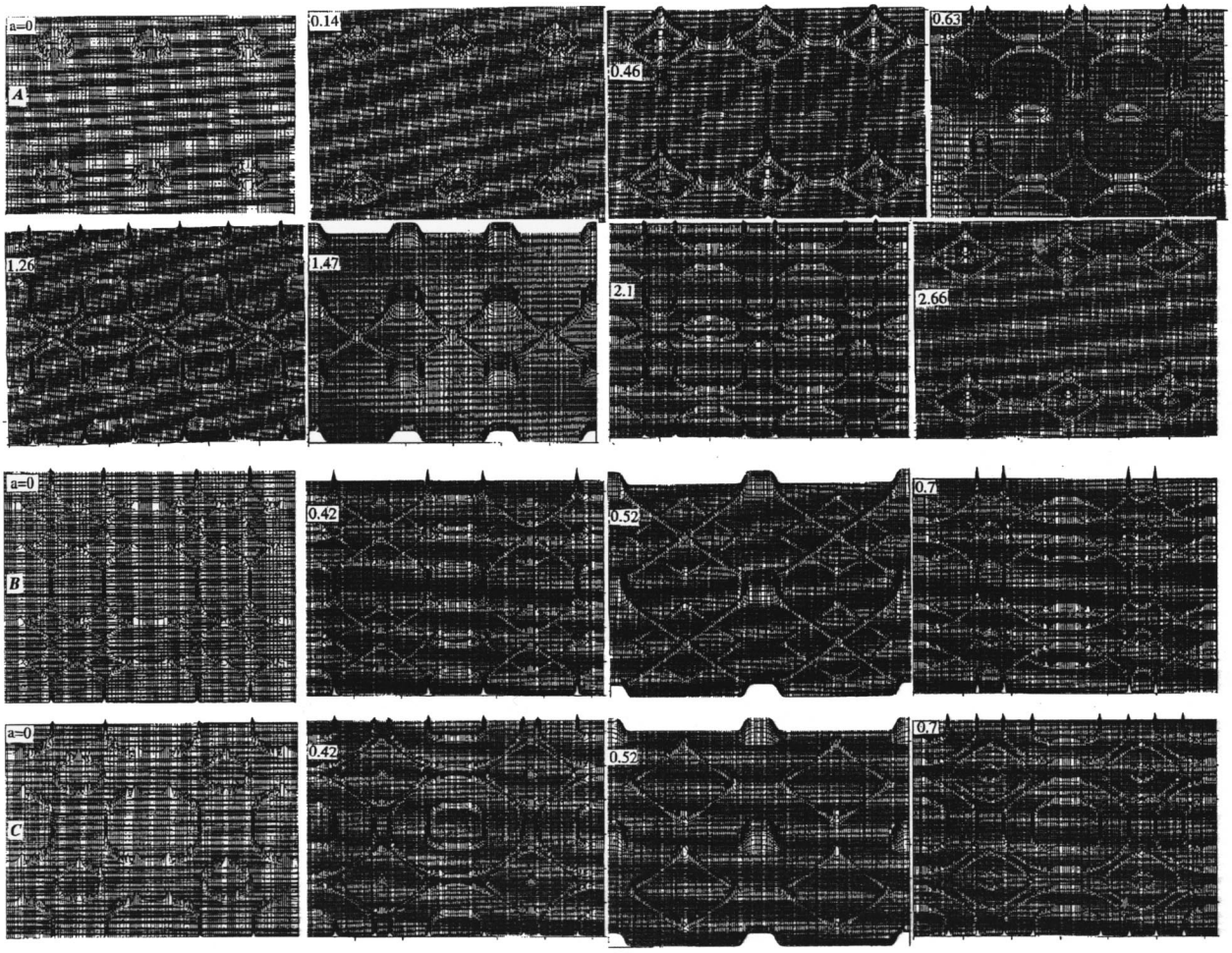

FIG. 14. Complex patterns [(a), (b), (c)] are formed by resonant traveling waves in x-y plane. Resonant conditions (38) take place for these waves. The generation, the interaction, the transformation, and the disappearance of localized structures are shown. According to the theory these processes are described by all equations (1)–(10). Perhaps, this figure simulates qualitatively the interaction of localized microwaves and vortices in some quantum fields during the period of oscillations. In particular, in the Bose–Einstein condensate experiments (Refs. 6, 90–93) this interaction may take place.

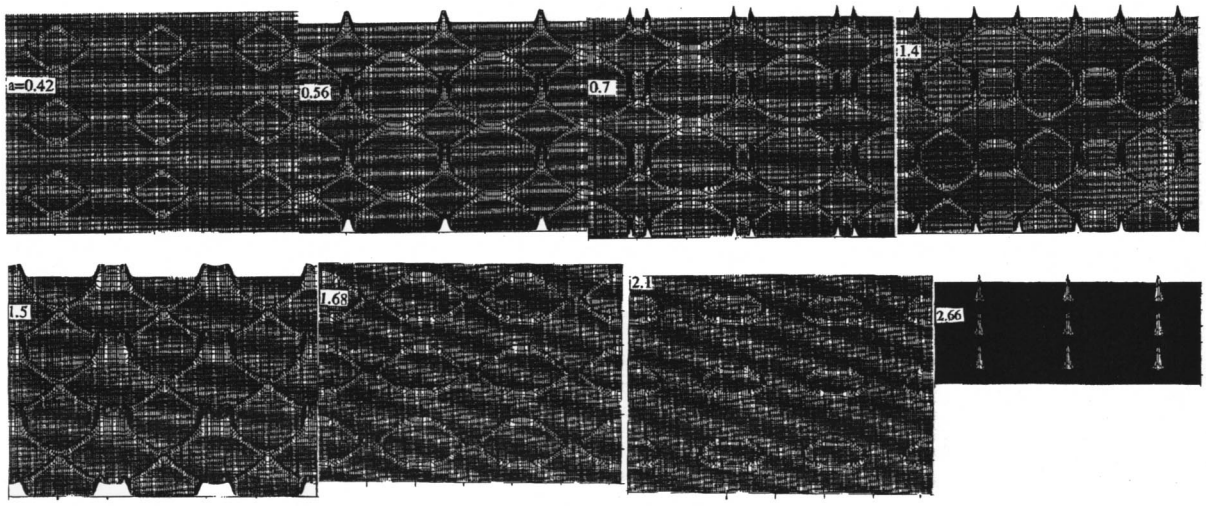

FIG. 15. Evolution of the resonant traveling wave patterns in x-y plane during the period of oscillations.

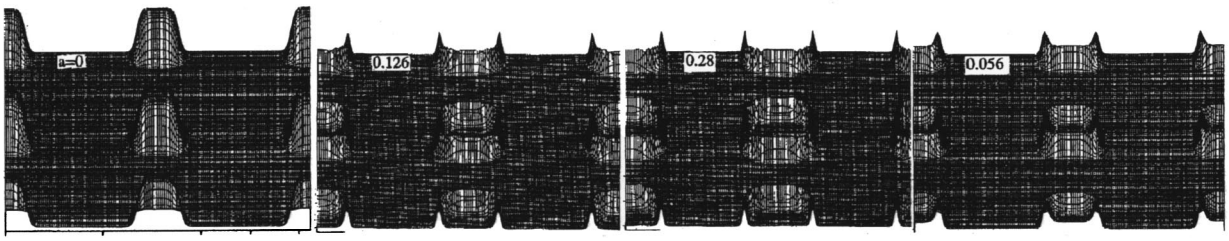

FIG. 16. The slow dynamics of oscillon-like structures formed by resonant traveling waves in x-y plane.

$$J'(r)=\mathrm{sech}^2(e\sin\zeta_-)\cos^2\zeta_-,$$
$$J'(s)=\mathrm{sech}^2(e\sin\zeta_+)\cos^2\zeta_+. \tag{52}$$

Here $\zeta_-=M^{-1}(r+c_-)$ and $\zeta_+=M^{-1}(s+c_+)$, where

$$r=a(t)-\sin^w k_1x+b^*\sin^v k_2y,$$
$$s=a(t)+\sin^w k_1x+\sin^v k_2y. \tag{53}$$

This case corresponds to resonant conditions (38). In this section dimensionless values r, s, ζ_-, ζ_+ and $a(t)$ are used. In (53) $a(t)$ is defined by parameters of the physical system. At the same time $a(t)$ defines the dynamics of wave patterns. Dynamic patterns are formed, if $a(t)>1$ [see Figs. 14, 15, 19(a), and 20]. If $a(t)\ll 1$, we have approximately the standing wave patterns (see Figs. 16 and 17).

Figure 14 demonstrates the complex dynamics of the patterns. Figure 14(a) was calculated for $b^*=-1$, $w=4$, $v=5$, $k_1=k_2=3$ in (53) and $c_\pm=0.5$, $e=30$ in (52). Figures 14(b) and 14(c) were calculated for $w=4$, $v=4$, $k_1=k_2=2$ in (53) and $c_\pm=0.5$, $M^{-1}=3$, $e=30$ in (52). In the last two cases, we only changed b^* [$b^*=1$ for Fig. 14(b) and $b^*=-1$ for Fig. 14(c)]. Then we recalculated Fig. 14(a) assuming that $w=4$, $v=4$, and $b^*=1$. Results are presented in Fig. 15. It is seen from Figs. 14(a) and 15 that the influence of w, v, and b^* on the wave patterns may be very strong.

Figures 14 and 15 manifest the traveling wave patterns. One can consider periodic generation, interaction, transformation, and disappearance of the localized elements during the dynamic process. Indeed, dynamical systems may exhibit complex behavior in both space and time.[70–73] In particular, time evolution of 1D and 2D standing wave patterns in different mechanical, optical, physical, chemical, and biological systems during one period have been treated.[53,55,74–76] Recently, highly dynamic patterns formed by traveling waves have attracted some attention.[21–27,77–79] We think that they can form in highly nonlinear, weakly dissipative media and in cavities with special boundaries. These conditions may be realized in microresonators.[80–83] On the other hand, the patterns in Figs. 14 and 15 recall the same patterns calculated for oscillatory and excitable media.[79,84] Very complex patterns similar to Figs. 14 and 15 are excited due to the interaction of boundaries and nonlinearity.[85] Circles and rings in Figs. 14–16 may be considered as vortices. Complex patterns formed by chains of vortices were observed recently.[86] The weak dynamics of the pattern is shown in Fig. 16. We used the parameters of Fig. 14(c) assuming additionally that $c_\pm=0$, $M^{-1}=1$ and $a(t)=0.28\sin\omega t$. A few sanding wave patterns are given in Fig. 17.

One can see that both dynamic and standing wave patterns can be formed from rolls, spots, circles, rings, squares, and hexagons. These elements of patterns are observed in the superconduction,[35,87] surface waves,[53,55,70,71] nonlinear optics,[72,73,88] and molecular,[76,89] Bose–Einstein condensate,[90–93] quantum[6–8] and biological systems.[70,74] Therefore Figs. 14–17 qualitatively describe many observed patterns.

Simulation of holes (vortices) in the Bose–Einstein condensate (BEC). BEC is formed when the temperature of atoms is very near absolute zero. In BEC all atoms lock together in one quantum mechanical state—as uniform and coherent as a single particle. In particular, they have the correlated spins. Recent experiments[6,90–93] show that a laser beam bounced in a resonator creates holes in BEC. Using the universal wave functions (52) we can qualitatively simulate these experiments. Results of calculations are presented in Fig. 18. We assumed that $a(t)=0$, $e=30$, $M^{-1}=1$, $c_\pm=0$, and $w=v=4$ in (52) and (53). One can see in Fig. 18 that the amount of holes (vortices) observed in Ref. 92 corresponds to numbers $k_1=1$, $k_2=1$ (one hole), $k_1=1$, $k_2=2$ (two holes), $k_1=2$, $k_2=2$ (four holes). Many holes shown in Refs. 6 and 90 were simulated by $k_1=4$, $k_2=4$ in (53).

Simulation of patterns in electron resonators (Refs. 7, 8, 94, 95) and photonic crystals (Refs. 72, 73, 88, 96–100). We assume that $J'(s)=0$, $e=5$, and

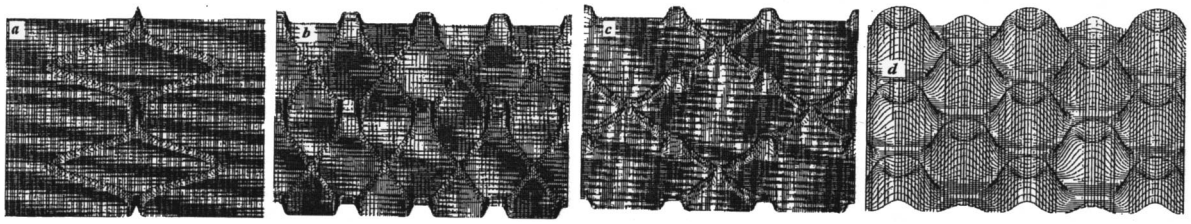

FIG. 17. Examples of simple resonant wave patterns in x-y plane calculated according to (52) and (53) for $a(t)=0$.

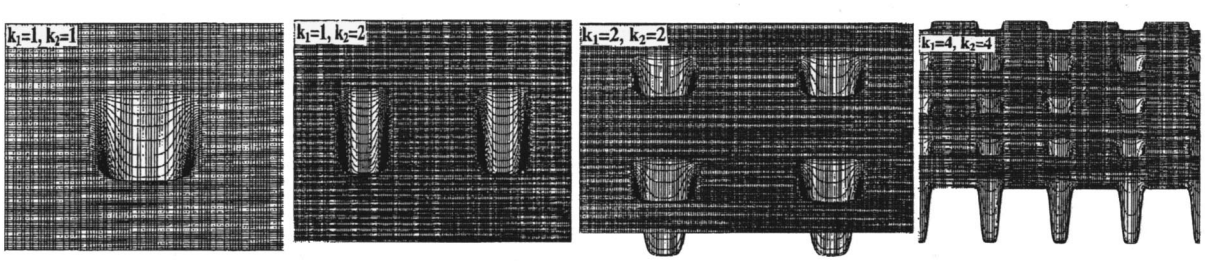

FIG. 18. Standing resonant wave patterns simulating holes and vortices observed in the Bose–Einstein condensate (Ref. 92). In the experiments (Refs. 6, 90–93) the amount of the vortices depended on the microwaves generated in the condensate. According to the theory this amount depended on the eigenvalues k_1 and k_2 of the universal function (52).

$$J'(r)=\mathrm{sech}^2(e\sin r)\cos^2 r, \tag{54}$$

$$r=1-a(t)-\mathrm{sech}(e_*R_*)\sin^N(k_1\varphi_*)-0.75\sin^N(k_2R_*)$$

in (53). Here $R_*=(\pi/L)(x^2+0.6y^2)^{0.5}-1$, $\varphi_*=\arctan(x/y)$, and e_* is a constant. Expression (54) satisfies resonant conditions (38). First we studied the Kondo resonance.[7,8] Figures 19(a)–19(c) demonstrate that expression (54) qualitatively describes the resonant standing wave patterns of a Kondo corral.[7] The dynamics of the quantum mirage observed in Ref. 7 is presented in Fig. 19(a). For the last case we assumed $e_*=30$, $k_1=16$, $k_2=12$, $N=4$ in (54). The form of the corral depends on e_* [see Fig. 19(b) calculated for $k_1=8$, $k_2=4$, $N=4$]. One can see that Figs. 19(a) and 19(b) also resemble the nonlinear optical phenomena and the photoelectron diffraction data published recently.[72,73,76,88,96–99] Assuming $r=1+\mathrm{sech}(e_*R_*)\times\sin^N(k_1\varphi_*)+0.75\sin^N(k_2R_*)$ in (54) and $k_1=8$, $e_*=2$ we simulated the last experimental data. The results of the calculations are presented in Fig. 19(c) for different k_2. One can see that Fig. 19(c) qualitatively simulates the optical patterns in cavities[72,73] and Kerr or resonant media.[96] Moreover, Fig. 19(c) describes qualitatively the mirages of atomic structures observed in Refs. 94, 95, and 98.

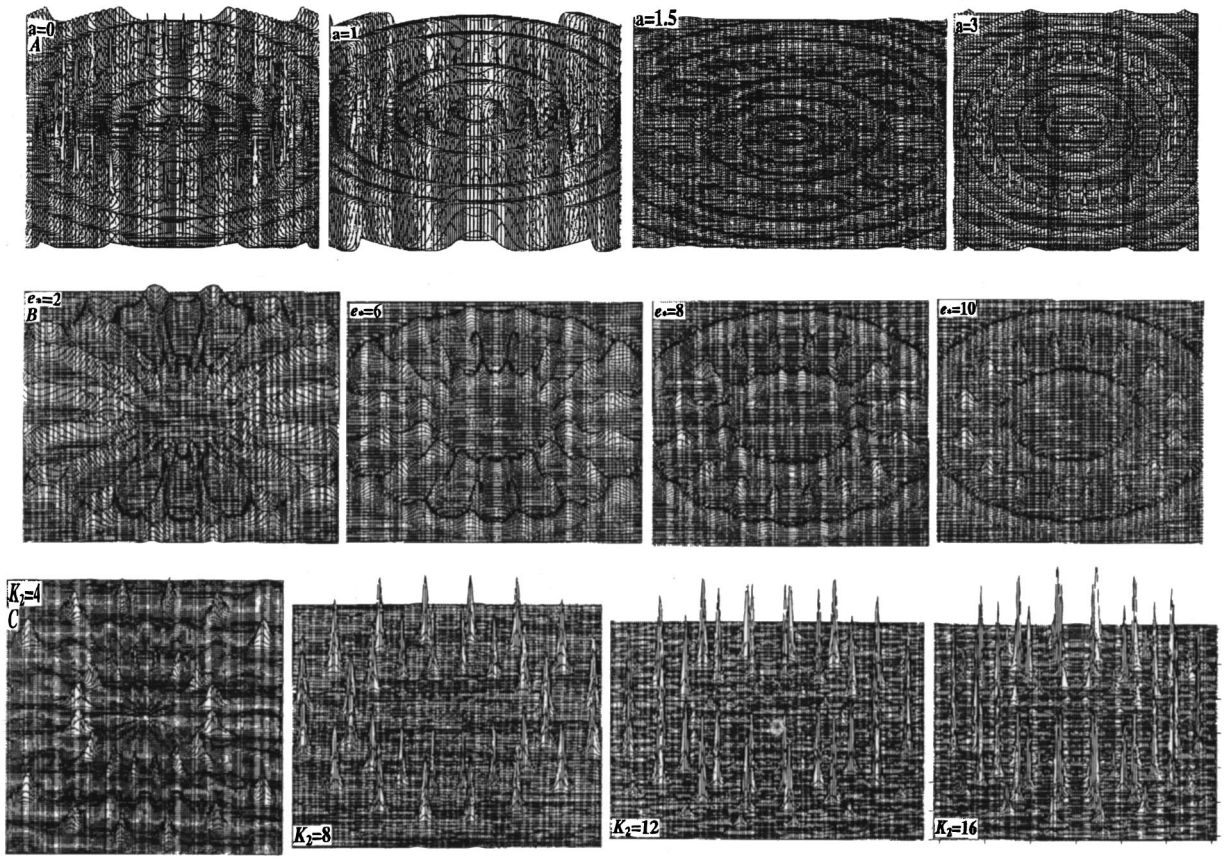

FIG. 19. Dynamical (a) and statistical properties (b), (c) of the universal wave function, and the qualitative simulation of quantum mirages observed in Refs. 7 and 8 and holograms of atoms (Refs. 94, 95, and 98). (a) A Kondo corral (Refs. 7 and 8) and the evolution of peaks and rings there during the period. (b) Form of a Kondo corral depends on the parameter e_*. (c) The dependence of 3D holographic images of some atoms (Refs. 94, 95, and 98) from eigenvalue k_2 of the universal function (52). Some features of the diffraction patterns (Ref. 99) are simulated.

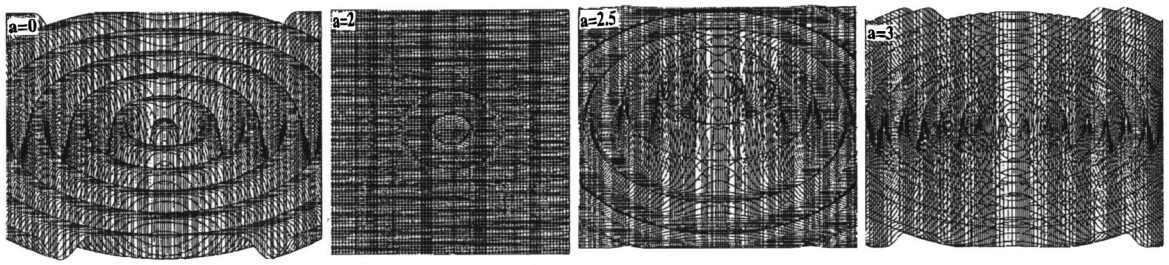

FIG. 20. Simulation of electron orbits in atoms (Refs. 97, 100, and 101) with the help of the universal wave function (52). The universal atomic electron's radial wave function varies during the period.

The dynamics of the orbit-like structures is shown in Fig. 20. We assumed in (54) that $r=-a(t)-0.75\,\mathrm{sech}(R_1)\sin^N(k_1R_*)$, where $R_1=(\pi/L)(1.2x^2+0.8y^2)^{0.5}$ and $k_2=10$. The orbits resemble the structures observed in different optical resonators.[97,100,101]

Thus, Figs. 18–20 simulate the different structures that are observed on the scale of atoms and electrons. In particular, Fig. 18 qualitatively describes holes and vortices in superconductors and BEC. Figures 19 and 20 demonstrate the wave functions of quantum particles. In one combination (Fig. 20) the electrons are smeared out in rings around the atom. In another (Fig. 19), they are localized and orbit around the atom like a planet around the sun. The electrons with high energy can occupy a large number of quantum states (Fig. 20). Moreover, Fig. 20 is a time sequence showing dynamics of the target patterns observed recently in oscillated granular layers.[102]

We recall that all states in Figs. 18–20 are described by the same wave function. This function also describes the liquid and granular waves in layers, seismic waves, and spherical waves. Therefore we consider function (49) as the universal function.[25,26]

V. CONCLUSIONS AND OPEN QUESTIONS

There are two main goals of this research. The first is to demonstrate the analogies between trans-resonant wave processes in different nonlinear, dispersive–dissipative systems. In particular, the analogies between surface waves, nonlinear and atom optics, field theories and acoustics of the early Universe are demonstrated. Second, it is the investigation of trans-resonant wave phenomena in these systems.

Some cases were found when the perturbed wave equations may be reduced to the basic highly nonlinear ordinary differential equation or the basic algebraic equation for traveling waves. The analytic solutions of these equations have been constructed. With the help of these solutions and the numerical calculations the 1D and 2D trans-resonant waves were studied. It is known[21–27] that in the trans-resonant frequency band the balance between the nonlinear, dispersive, dissipative, and spatial effects varies with the frequency. We found here that the harmonic waves can evolve into shock-, jet-, or mushroom-like waves, and then into cloud-like and vortex-like structures. Sometimes the motion of these waves and structures in the x–t and x–y planes may be very complex. They can form different traveling wave patterns.

We have shown that the above-mentioned trans-resonant waves and patterns qualitatively describe many recent observations. On the one hand, they simulate vertically excited surface waves in liquid and granular layers (the Faraday experiment). On the other hand, they describe nonlinear wave effects in optics. Moreover, we found that the analytic solutions (52) and (54) qualitatively describe wave patterns in Bose–Einstein condensates (Fig. 18), and the Kondo corrals observed recently in atom–electron structures (Fig. 19).

The results may be interpreted for different resonators and media. For example, according to Figs. 8–13, when the trans-resonant parameter R varies from $+1$ to -1, the harmonic ripples amplify and transform into the spiral and ellipsoidal structures, and the clusters of these structures. Perhaps this evolution describes the generation of galaxies, and the formation of galaxy clusters during the early Universe evolution. We believe that the condition $R\approx-1$ qualitatively characterizes moments of time and points of space in the early Universe, where galaxies and the clusters were formed. According to the presented analytic theory galaxies and galactic clusters were formed at the same time.

Figures 1–5 and 7 show the resonant localization and the compression of the forced harmonic excitation inside of the resonant band. Due to the parametric excitation the wave may be trapped. The wave can change the velocity and the direction of the motion (Figs. 1 and 2). The compression of the waves is maximal when $R\approx-1$. The resonant compression of harmonic waves, the localization of the waves, and the manipulation of the wave velocity realized in the microresonators (nanocrystals, molecules and atoms) may be used in quantum computing. The generation and the transformation of mushroom-like waves were studied. It is known that turbulence may be generated by mushroom-like waves.[65,66] We found that the mushroom-like waves and the spiral-like vortices can be generated by the fifth-order nonlinearity or the cubic nonlinearity together with the ''eddy'' viscosity (Figs. 8–13). Thus, the high nonlinearity can qualitatively simulate ''eddy'' viscosity and, perhaps, describes a generation of the wave turbulence. According to the theory the wave turbulence can weakly depend on the viscosity.

The standing wave patterns were intensively studied during the last decades.[55,70–74,76,103,104] We have considered the dynamic wave patterns. In particular, the analytic theory of patterns, which are formed by the trans-resonant traveling waves, have been developed. As a result, we simulated the

patterns which were observed recently in different quantum, electron, and atom systems.[6,7,90–100]

A detailed study of different trans-resonant wave phenomena can greatly clarify dynamic aspects of nonlinearity and the role they play in effects ranging from physics to biology. In particular, waves generated in nonlinear resonant bands[105,106] are weakly studied. Passing through resonance can strictly depend on noise. This problem was considered with the help of ordinary differential equations.[107] Apparently, stochastic trans-resonant nonlinear waves are the problem of the future. Subharmonic and high-harmonic waves may be generated in the resonant bands.[24,25,56,104,108] Further open questions are as follows.

(1) We took into account nonlinear, dispersive, dissipative, and spatial effects. Are they enough to describe all physical phenomena in resonant systems? Can they describe effects of the virtual particles and the Casimir force[109] in microelectromechanical resonant systems?

(2) One can see that waves in Figs. 14, 15, 19(a), and 20 can periodically disappear and generate. This process was observed in water[53,78] and granular layers.[55] Can this physical process correspond to the generation of resonant particles by fields? If $R \approx 1$ then the mushroom-like waves can generate the jets, and the cloud-like structures. In particular, we have connected this process with the formation of galaxy clusters. Can this process describe qualitatively the generation of the virtual particles in fields?

(3) It follows from the theory that highly nonlinear resonant fields may form vortices. The highly nonlinear fields and materials were found recently.[5,83] Is it possible that there the wave fields are formed by the vortices? Can this possibility explain properties of superconductors and the Bose–Einstein condensate?

(4) Figure 20 resembles the well known, in quantum mechanics, Wigner function.[101] Is function (54) some analog of the Wigner function?

(5) It is known that the versions[68,69] of Eq. (40) describe the chaotic oscillations in the resonant band. Indeed, if $R \approx -1$, then the strictly different roots locate very close to each other (see Figs. 9–11 and 13). In this case nonzero fluctuations can provoke the highly unpredictable bifurcations and jumps in the systems. These high nonlinear phenomena may be extremely important. Have we considered the systems stable to very small fluctuations? Can very small fluctuations of the parameters move the resonant systems from stable to unstable state and vice versa, if $R \approx -1$? Is it possible that the spatiotemporally deterministic mushroom-like waves,[65,66,110] spiral, and ellipsoidal vortices pass to turbulence without the above-mentioned linear process?

(6) It is known that large vortex structures may be considered as weakly viscous.[111] We qualitatively showed that the fifth-order nonlinearity [Eq. (1)] yields the vortex structures. Is it possible to use highly nonlinear wave equations and weakly viscous models [e.g., (1)] for studying of the large scale wave turbulence instead of the Navier–Stokes equations?

(7) Equation (1) was derived for highly elastic objects. According to the resonant solutions the vortices may be generated there. Can these solutions describe so-called ''elastic'' turbulence?[112,113]

(8) Is it possible to find in the theory of turbulent flow[47,61,114] or wave turbulence[115] some value which resembles the trans-resonant parameter R?

(9) Generally speaking in Sec. IV C we considered only one analytic solution of Eq. (40). Do solutions (46), (47), (48), and (50) describe some resonant properties of fields and microresonators?

(10) We showed that harmonic waves, shock-like waves, jets, mushroom-like waves and vortices can evolve into each other during the trans-resonant process. The similar evolution was observed in water and gas layers.[65,66,116,117] Perhaps, this process may be connected with a formation of quantum shock waves and a nucleation of vortices in BEC.[118] It follows from the theory and the observations that wave phenomena in the different media and the quantum effects in BEC may be similar. On the other hand, further analysis of the trans-resonant evolution of waves may be important the inflationary theory. This theory predicts that gravitational waves in the early Universe would have produced a vortex-like component.[119] Perhaps, this component might be generated due to the nonlinear trans-resonant evolution of harmonic gravitational waves. Might the nonlinear trans-resonant theory of gravitational waves tell whether inflation is right or not? Can the resonant waves and the nonlinear trans-resonant evolution of ripples into vortices illustrate properties of quantum waves, oscillating BEC[120] and the Universe?

ACKNOWLEDGMENTS

We are thankful to Professor A. V. Shanin for his critique. We appreciate useful comments from Professor D. Abbott and the anonymous reviewers.

[1] O. M. Phillips, J. Fluid Mech. **106**, 215 (1981).
[2] M. A. Ilgamov, R. G. Zaripov, R. G. Galiullin, and V. B. Repin, Appl. Mech. Rev. **49**, 137 (1996).
[3] O. V. Rudenko and A. V. Shanin, Acoust. Phys. **46**, 334 (2000).
[4] L. L. Sohn, Nature (London) **394**, 131 (1998).
[5] L. V. Hau, S. E. Harris, Z. Dutton, and C. H. Behroozi, Nature (London) **397**, 594 (1999).
[6] R. Fitzgerald, Phys. Today **8**, 19 (2000).
[7] H. C. Manoharan, C. P. Lutz, and D. M. Elgler, Nature (London) **403**, 512 (2000).
[8] G. A. Fiete, J. S. Hersch, E. J. Heller, H. C. Manoharan, C. P. Lutz, and D. M. Elgler, Phys. Rev. Lett. **86**, 2392 (2001).
[9] J. C. Bronski, L. D. Carr, B. Deconinck, J. N. Kutz, and K. Promislow, Phys. Rev. E **63**, 036612 (2001).
[10] J. Magueijo, Sci. Am. **284** (N1), 46 (2001).
[11] R. A. Sunyaev and Ya. B. Zeldovich, Astron. Astrophys. **20**, 189 (1972).
[12] R. A. Sunyaev and Ya. B. Zeldovich, Astrophys. Space Sci. **7**, 3 (1970).
[13] S. F. Shandarin and Ya. B. Zeldovich, Rev. Mod. Phys. **61**, 185 (1989).
[14] P. J. E. Peebles, *The Large-Scale Structure of the Universe* (Princeton University Press, Princeton, 1980).
[15] S. D. M. White, J. F. Navarro, A. E. Evrard, and C. S. Frenk, Nature (London) **366**, 429 (1993).

[16] S. D. M. White, in *Cosmology and Large-scale Structure, Proceedings of the 60th Les Houches School*, edited by R. Schaeffer, J. Silk, M. Spiro, and J. Zinn-Justin (Elsevier, Amsterdam, 1997), p. 349.
[17] L. M. Krauss, Sci. Am. **280** (N1), 35 (1999).
[18] M. J. Rees, Science **290**, 1919 (2000).
[19] P. Coles and L.-Y. Chiang, Nature (London) **406**, 376 (2000).
[20] C. Seife, Science **291**, 414 (2001).
[21] Sh. U. Galiev and T. Sh. Galiev, Strength Mater. **9**, 633 (1994).
[22] Sh. U. Galiev and T. Sh. Galiev, Phys. Lett. A **246**, 299 (1998).
[23] Sh. U. Galiev, Phys. Lett. A **260**, 225 (1999).
[24] Sh. U. Galiev, J. Phys. A **32**, 6963 (1999).
[25] Sh. U. Galiev, Phys. Lett. A **266**, 41 (2000).
[26] Sh. U. Galiev, in *Unsolved Problems of Noise and Fluctuations*, edited by D. Abbott and L. B. Kish (American Institute of Physics, New York, 2000), Vol. 511, p. 361.
[27] Sh. U. Galiev, Geophys. J. Int. (accepted).
[28] Sh. U. Galiev, Izv. Acad. Nauk USSR, Mech. Solid Body **4**, 80 (1972).
[29] Sh. U. Galiev, *Nonlinear Waves in Bounded Continua* (Naukova Dumka, Kiev, 1988) (in Russian).
[30] S. M. Bezrukov and I. Vodyanoy, Nature (London) **385**, 319 (1997).
[31] M. Remoissenet, *Waves Called Solitons* (Springer, New York, 1996).
[32] R. K. Bullough, P. M. Jack, P. W. Kitchenside, and R. Saunders, Phys. Scr. **20**, 364 (1979).
[33] F. K. Kneubühl, *Oscillations and Waves* (Springer, Berlin, 1997).
[34] T. I. Belova and A. E. Kudryavtsev, Phys. Usp. **40**, 359 (1997).
[35] C. C. Tsuei and J. R. Kirtley, Rev. Mod. Phys. **72**, 969 (2000).
[36] Z. F. Ezawa, *Quantum Hall Effects* (World Scientific, Singapore, 2000).
[37] A. R. Liddle and D. H. Lyth, *Cosmological Inflation Large-Scale Structure* (Cambridge University Press, Cambridge, 2000).
[38] E. Harrison, *Cosmology* (Cambridge University Press, Cambridge, 2000).
[39] W. Hu, R. Barkana, and A. Gruzinov, Phys. Rev. Lett. **85**, 1158 (2000).
[40] A. Vilenkin and E. P. S. Shellard, *Cosmic Strings and other Topological Defects* (Cambridge University Press, Cambridge, 1994).
[41] V. Méndez, J. Fort, and J. Farjas, Phys. Rev. E **60**, 5231 (1999).
[42] I. A. Ivonin, V. P. Pavlenko, and H. Persson, Phys. Rev. E **60**, 492 (1999).
[43] Sh. U. Galiev, in *Proceedings of the Thirteenth Australasian Fluid Mechanics Conference*, edited by M. C. Thompson and K. Hourigan (Monash University, Melbourne, 1998), p. 1027.
[44] W. Chester and A. Moser, Proc. R. Soc. London, Ser. A **380**, 409 (1982).
[45] K. R. Sreenivasan, Rev. Mod. Phys. **71**, S383 (1999).
[46] L. van Wijngaarden, J. Eng. Math. **2**, 225 (1968).
[47] M. Kardar and R. Golestanian, Rev. Mod. Phys. **71**, 1233 (1999).
[48] P. C. W. Davies, in *Unsolved Problems of Noise and Fluctuations*, edited by D. Abbott and L. B. Kish (American Institute of Physics, New York, 2000), Vol. 511, p. 16.
[49] N. N. Akhmediev, Opt. Quantum Electron. **30**, 535 (1998).
[50] X. Wang and R. Wei, Phys. Lett. A **192**, 1 (1994).
[51] X. Wang and R. Wei, Phys. Rev. Lett. **78**, 2744 (1997).
[52] D. E. Rourke and M. P. Augustine, Phys. Rev. Lett. **84**, 1685 (2000).
[53] O. Lioubashevski, Y. Hamiel, A. Agnon, Z. Reches, and J. Fineberg, Phys. Rev. Lett. **83**, 3190 (1999).
[54] M. S. Longuet-Higgins, J. Fluid Mech. **127**, 103 (1983).
[55] P. B. Umbanhowar, F. Melo, and H. L. Swinney, Nature (London) **382**, 793 (1996).
[56] L. Jiang, M. Perlin, and W. W. Schultz, J. Fluid Mech. **369**, 273 (1998).
[57] B. W. Zeff, B. Kleber, J. Fineberg, and D. L. Lathrop, Nature (London) **403**, 401 (2000).
[58] D. E. Kataoka and S. M. Troian, Nature (London) **402**, 794 (1999).
[59] C. L Goodridge, W. T. Shi, H. G. E. Hentschel, and D. P. Lathrop, Phys. Rev. E **56**, 472 (1997).
[60] A. M. Jellinek, R. C. Kerr and R. W. Griffiths, in *Proceedings of the Thirteenth Australasian Fluid Mechanics Conference*, edited by M. C. Thompson and K. Hourigan (Monash University, Melbourne, 1998), p. 1023.
[61] T. E. Faber, *Fluid Dynamics for Physicists* (Cambridge University Press, Cambridge, 1995).
[62] D. Morton, M. Rudman, and J.-L. Liow, in *Proceedings of the Thirteenth Australasian Fluid Mechanics Conference*, edited by M. C. Thompson and K. Hourigan (Monash University, Melbourne, 1998), p. 949.
[63] A. Frohn and N. Roth, *Dynamics of Droplets* (Springer, New York, 2000).
[64] V. Bergeron, D. Bonn, J. Y. Martin, and L. Vovelle, Nature (London) **405**, 772 (2000).
[65] C. Suplee, *Physics in the 20th Century* (Abrams, New York, 1999).
[66] K. Prestridge, P. Vorobieff, P. M. Rightley, and R. F. Benjamin, Phys. Rev. Lett. **84**, 4353 (2000).
[67] G. I. Taylor, Proc. R. Soc. London, Ser. A **164**, 476 (1938).
[68] R. Grimshaw and X. Tian, Proc. R. Soc. London, Ser. A **445**, 1 (1994).
[69] J. M. T. Thompson, Appl. Mech. Rev. **50**, 307 (1997).
[70] M. C. Cross and P. C. Hohenberg, Rev. Mod. Phys. **65**, 851 (1993).
[71] K. J. Lee and H. L. Swinney, Phys. Rev. E **51**, 1899 (1995).
[72] L. A. Lugiato, M. Brambilla, and A. Gatti, Adv. At., Mol., Opt. Phys. **40**, 229 (1999).
[73] F. T. Arecci, S. Boccaletti, and P. L. Ramazza, Phys. Rep. **318**, 1 (1999).
[74] H. D. Walgraef, *Spatio-Temporal Pattern Formation* (Springer, New York, 1997).
[75] H.-J. Pi, S.-Y. Park, J. Lee, and K. J. Lee, Phys. Rev. Lett. **84**, 5316 (2000).
[76] *The Handbook of Surface Imaging and Visualization*, edited by A. T. Hubbard (CRC Press, Boca Raton, FL, 1995).
[77] E. Cerda, F. Melo, and S. Rica, Phys. Rev. Lett. **79**, 4570 (1997).
[78] O. Lioubashevski and J. Fineberg, Phys. Rev. E **63**, 035302 (2001).
[79] Q. Quyang, H. L. Swinney, and G. Li, Phys. Rev. Lett. **84**, 1047 (2000).
[80] P. W. H. Pinkse, T. Fischer, P. Maunz, and G. Rempe, Nature (London) **404**, 365 (2000).
[81] C. J. Hood, T. W. Lynn, A. C. Doherty, A. S. Parkins, and H. J. Kimble, Science **287**, 1447 (2000).
[82] K.-D. Liss, R. Hock, M. Gomm, B. Waibel, A. Magerl, M. Krisch, and R. Tucoulou, Nature (London) **404**, 371 (2000).
[83] H. Kishida, H. Matsuzaki, H. Okamoto, T. Nanabe, M. Yamashita, Y. Taquchi, and Y. Tokura, Nature (London) **405**, 923 (2000).
[84] S. Komineas, F. Heilmann, and L. Kramer, Phys. Rev. E **63**, 011103 (2001).
[85] A. Kidrolli, M. C. Abraham, and J. P. Gollub, Phys. Rev. E **63**, 026208 (2001).
[86] J. Zhang, S. Childress, A. Libchaber, and M. Shelley, Nature (London) **408**, 835 (2000).
[87] L. F. Chibotaru, A. Ceulemans, V. Bruyndonex, and V. V. Moshchalkov, Phys. Rev. Lett. **86**, 1323 (2001).
[88] M. Mitchell and M. Segev, Nature (London) **387**, 880 (1997).
[89] G. Guttroff, M. Bayer, A. Forchel, P. A. Knipp, and T. L. Reinecke, Phys. Rev. E **63**, 036611 (2001).
[90] D. Voss, Science **291**, 2301 (2001).
[91] M. R. Matthews, B. P. Anderson, P. C. Haljan, D. S. Hall, C. E. Wieman, and E. A. Cornell, Phys. Rev. Lett. **83**, 2498 (1999).
[92] K. W. Madison, F. Chevy, W. Wohlleben, and J. Dalibard, Phys. Rev. Lett. **84**, 806 (2000).
[93] R. Onofrio, D. S. Durfee, C. Raman, M. Köhl, C. E. Kuklewicz, and W. Ketterle, Phys. Rev. Lett. **84**, 810 (2000).
[94] J. Spence, Nature (London) **410**, 1037 (2001).
[95] J. Wider, F. Baumberger, M. Sambi, R. Gotter, A. Verdini, F. Bruno, D. Cvetko, A. Morgante, T. Greber, and J. Osterwalder, Phys. Rev. Lett. **86**, 2337 (2001).
[96] S. G. Odoulov, M. Yu. Goulkov, and O. A. Shinkarenko, Phys. Rev. Lett. **83**, 3637 (1999).
[97] M. Campbell, D. N. Sharp, M. T. Harrison, R. G. Denning, and A. J. Turberfield, Nature (London) **404**, 53 (2000).
[98] P. Korecki and G. Materlik, Phys. Rev. Lett. **86**, 2333 (2001).
[99] S. Dreiner, M. Schürmann, C. Westphal, and H. Zacharias, Phys. Rev. Lett. **86**, 4068 (2001).
[100] M. Vaupel, A. Maitre, and C. Fabre, Phys. Rev. Lett. **83**, 5278 (1999).
[101] W. P. Schleich, *Quantum Optics in Phase Space* (Wiley-VCH, New York, 2001).
[102] J. R. de Bruyn, B. C. Lewis, M. D. Shattuck, and H. L. Swinney, Phys. Rev. E **63**, 041305 (2001).
[103] H. M. Jaeger, S. R. Nagel, and R. P. Behringer, Rev. Mod. Phys. **68**, 1259 (1996).
[104] W. X.-L. Wang, Y.-H. Chen, and R.-J. Wei, Chin. Phys. Lett. **17**, 580 (2000).
[105] Sh. U. Galiev, M. A. Ilgamov, and A. V. Sadikov, Izv. Acad. Nauk USSR, Mech. Fluid and Gas **2**, 57 (1970).
[106] Sh. U. Galiev, Izv. Acad. Nauk USSR, Mech. Solid Body **1**, 58 (1972).
[107] J. C. Celet, D. Dangoisse, P. Glorieux, G. Lythe, and T. Erneux, Phys. Rev. Lett. **81**, 975 (1998).
[108] A. L. Lin, M. Bertram, K. Martinez, and H. L. Swinney, Phys. Rev. Lett. **84**, 4240 (2000).
[109] H. B. G. Casimir, Proc. K. Ned. Akad. Wet. B **51**, 793 (1948).
[110] R. L. Holmes, G. Dimonte, B. Fryxell, M. L. Gittings, J. W. Grove, M.

Schneider, D. H. Sharp, A. L. Velikovich, R. P. Weaver, and Q. Zhang, J. Fluid Mech. **389**, 55 (1999).
[111] L. D. Landau and E. M. Lifshitz, *Fluid Mechanics* (Pergamon, New York, 1987).
[112] R. G. Larson, Nature (London) **405**, 27 (2000).
[113] M. Chertkov, Phys. Rev. Lett. **84**, 4761 (2000).
[114] G. I. Barenblatt, A. J. Chorin, and V. M. Prostokishin, Appl. Mech. Rev. **50**, 413 (1997).
[115] D. Cai, A. J. Majda, D. W. Mclaughlin, and E. G. Tabak, PNAS **96**, 14216 (1999).
[116] W. Chester and J. A. Bones, Proc. R. Soc. London, Ser. A **306**, 23 (1968).
[117] A. S. Sabry and J. T. Liu, J. Fluid Mech. **231**, 615 (1991).
[118] Z. Dutton, M. Budde, C. Slowe, and L. V. Hau, Science **293**, 663 (2001).
[119] C. Seife, Science **292**, 2236 (2001).
[120] P. Ball, Nature (London) **411**, 628 (2001).